AMERICAN SOCIETY FOR MICROBIOLOGY | Microbiology Resource Announcements

GENOME SEQUENCES

Draft Genome Sequences of Two Clinical Mastitis-Associated *Escherichia coli* Strains, of Sequence Type 101 and Novel Sequence Type 13054, Isolated from Dairy Cows in Bangladesh

Mohammad H. Rahman,[a] Mohamed E. El Zowalaty,[b] Linda Falgenhauer,[c,d,e] Mohammad Ferdousur Rahman Khan,[a] Jahangir Alam,[f] Najmun Nahar Popy,[a] M. Bahanur Rahman[a]

[a]Department of Microbiology and Hygiene, Bangladesh Agricultural University, Mymensingh, Bangladesh
[b]Veterinary Medicine and Food Security Research Group, Medical Laboratory Sciences Program, Faculty of Health Sciences, Abu Dhabi Women's Campus, Higher Colleges of Technology, Abu Dhabi, United Arab Emirates
[c]German Center for Infection Research, Site Giessen-Marburg-Langen, Giessen, Germany
[d]Institute of Hygiene and Environmental Medicine, Justus Liebig University Giessen, Giessen, Germany
[e]Hessian University Competence Center for Hospital Hygiene, Justus Liebig University Giessen, Giessen, Germany
[f]National Institute of Biotechnology, Savar, Dhaka, Bangladesh

Mohammad H. Rahman and Mohamed E. El Zowalaty are equal first authors and were arranged by order of increasing seniority.

ABSTRACT Here, we report the draft genome sequences of two *Escherichia coli* strains that were isolated from raw milk samples obtained from lactating cows with mastitis in Bangladesh. One strain was assigned to a novel sequence type 13054, and the other strain belonged to sequence type 101.

Mastitis is a complex, multi-etiological disease caused by more than 140 bacterial species. It is one of the most widespread diseases of major economic importance in the dairy industry worldwide (1, 2). *Escherichia coli* is one of the leading mastitis-causing pathogens (2–5). Mastitis is a disease with serious zoonotic potential associated with shedding of bacteria and their toxins, including Shiga toxin-producing *E. coli* strains (6), through unpasteurized milk, constituting potential threats to humans and other animals. Here, we report the draft genome sequences of two *E. coli* strains that were isolated from raw milk samples obtained from lactating cows with mastitis in Bangladesh. The study was performed due to the lack of genome-based studies of mastitis-causing *E. coli* strains from Bangladesh.

Mastitis milk samples (10 mL) that had been collected in sterile tubes from 36-month and 46-month-old lactating Holstein-Friesian cows (*Bos taurus taurus*) were transported to the laboratory, maintaining a proper cold chain. Nutrient broth (10 mL) was inoculated with 500 μL of a milk sample, incubated at 37°C for 18 h, and subsequently streaked on selective eosin methylene blue (EMB) agar plates (HiMedia Laboratories LLC., Mumbai, India). After incubation at 37°C for 24 h, pure single colonies were identified as *E. coli* using Gram staining and the indole, methyl red, Voges-Proskauer, citrate utilization (IMViC) test. The purified cultures of the two *E. coli* strains were submitted to Invent Technology Ltd. (Banani, Dhaka, Bangladesh) for whole genome sequencing. DNA was extracted from overnight cultures that had been grown in nutrient broth at 37°C, using a genomic DNA purification kit (Promega, WI, USA). Sequencing libraries were prepared using the Nextera XT library preparation kit (Illumina, CA, USA) and were sequenced on an Illumina NextSeq 550 system using the NextSeq 500/550 high-output kit v2.5 (300 cycles).

Default parameters were used for all software unless otherwise specified. Quality control was performed using ASA^{3}P v1.4.0 (7). Assembly was performed using SPAdes v3.13.0 (8) integrated in ASA^{3}P. Contigs, excluding those smaller than 200 bp, were uploaded to the National Center

Editor David Rasko, University of Maryland School of Medicine

Address correspondence to Mohamed E. El Zowalaty, elzow005@gmail.com, or M. Bahanur Rahman, bahanurr@bau.edu.bd.

The authors declare no conflict of interest.

Received 3 March 2023
Accepted 13 May 2023

TABLE 1 Basic characteristics of the whole-genome sequencing, assembly, and annotation of strains BR-MHR261 and BR-MHR268 reported in the present study

	Finding for strain:	
Parameter	**BR-MHR261**	**BR-MHR268**
No. of raw reads	17,971,212	19,625,988
Avg read length (nucleotides)	128.9	129
Avg coverage (×)	462	518
No. of contigs of >200 bp	93	152
N_{50} (bp)	212,731	217,132
Genome size (bp)	5,014,182	4,887,493
G+C content (%)	50.6	50.6
Total no. of genes	4,929	4,831
No. of coding sequences (with protein)	4,701	4,586
No. of RNA genes	87	86
No. of rRNAs (5S, 16S, 23S)	1, 1, 2	0, 2, 1
No. of complete rRNAs (5S, 16S, 23S)	1, 1, 0	0, 0, 1
No. of partial rRNAs (5S, 16S, 23S)	0, 0, 1	0, 2, 1
No. of tRNAs	75	74
No. of noncoding RNAs	8	9
No. of pseudogenes (total)	142	159

for Biotechnology Information (NCBI) (Bethesda, MD, USA) and annotated using the NCBI Prokaryotic Genome Annotation Pipeline (PGAP) v6.0 (9). Sequencing, assembly, and annotation data for BR-MHR261 and BR-MHR268 are summarized in Table 1.

No antibiotic resistance genes were detected using ResFinder v4.0 (10). Virulence genes detected with the Virulence Factor Database (VFDB) integrated in ASA^{3}P differed in the two isolates. BR-MHR261 and BR-MHR268 harbored 46 and 34 virulence determinants, respectively. Both isolates harbored genes involved in iron acquisition (enterobactin) and the *E. coli* common pilus. Unique features were type II secretion system genes in BR-MHR261 and type I fimbria genes in BR-MHR268.

Multilocus sequence typing (MLST) sequence types (STs) were determined using PubMLST (11) and the Achtman scheme (12). BR-MHR261 had a new and very rare ST (ST-13054). BR-MHR268 was an ST-101 isolate. *E. coli* ST-101 strains have already been detected in mastitis samples (13).

This report highlights the significance of continued genomic surveillance of mastitis-associated *E. coli* in food chain cattle and food production, which will help us to understand its role in the spread of antimicrobial resistance and pathogenesis.

Data availability. This whole-genome sequencing project has been deposited in DDBJ/ENA/GenBank under the accession numbers JALBGL000000000 (BR-MHR261) and JALBGK000000000 (BR-MHR268). The versions described here are the first versions. The sequences are publicly available under BioProject accession number PRJNA716986, BioSample accession numbers SAMN26025966 (BR-MHR261) and SAMN26025967 (BR-MHR268), and SRA accession numbers SRR18182111 (BR-MHR261) and SRR18182110 (BR-MHR268). All genomes are also publicly available at PubMLST (https://pubmlst.org/organisms/escherichia-spp).

ACKNOWLEDGMENTS

The whole-genome sequencing work was supported in part by the Bangladesh Academy of Sciences and the U.S. Department of Agriculture (project BAS-USDA LS-26/2020), the Bangladesh Agricultural University Research System (BAURES), and the Hessian Ministry of Higher Education, Research, and Arts (Germany) within the project Hessisches Universitaeres Kompetenzzentrum Krankenhaus Hygiene (HuKKH).

We thank the NCBI GenBank submission staff for help with the genome uploading, decontamination, and deposition process. We thank Keith Jolley, PubMLST *E. coli* curator, from the Department of Zoology, University of Oxford (Oxford, UK), for his help. We thank the anonymous reviewer for the insightful comments that significantly improved the manuscript.

The views, opinions, and/or findings expressed are those of the authors and should not be interpreted as representing the official views or policies of the U.S. Department of Agriculture or the U.S. Government.

M.H.R., M.B.R., and M.E.Z. designed the experiment. M.H.R., M.F.R.K., J.A., and N.N.P. performed sample collection, bacterial culture and preliminary identification of the samples. L.F. analyzed the genomes. L.F. and M.E.Z. analyzed the data and wrote the announcement manuscript. M.E.Z. critically revised the manuscript. M.B.R. and M.E.Z. supervised the project.

REFERENCES

1. Goulart DB, Mellata M. 2022. *Escherichia coli* mastitis in dairy cattle: etiology, diagnosis, and treatment challenges. Front Microbiol 13:928346. https://doi.org/10.3389/fmicb.2022.928346.
2. Pascu C, Herman V, Iancu I, Costina L. 2022. Etiology of mastitis and antimicrobial resistance in dairy cattle farms in the western part of Romania. Antibiotics 11:57. https://doi.org/10.3390/antibiotics11010057.
3. Al-Harbi H, Ranjbar S, Moore RJ, Alawneh JI. 2021. Bacteria isolated from milk of dairy cows with and without clinical mastitis in different regions of Australia and their AMR profiles. Front Vet Sci 8:743725. https://doi.org/10.3389/fvets.2021.743725.
4. Cheng WN, Han SG. 2020. Bovine mastitis: risk factors, therapeutic strategies, and alternative treatments: a review. Asian-Australas J Anim Sci 33:1699–1713. https://doi.org/10.5713/ajas.20.0156.
5. Dalanezi FM, Joaquim SF, Guimarães FF, Guerra ST, Lopes BC, Schmidt EMS, Cerri RLA, Langoni H. 2020. Influence of pathogens causing clinical mastitis on reproductive variables of dairy cows. J Dairy Sci 103:3648–3655. https://doi.org/10.3168/jds.2019-16841.
6. Murinda SE, Ibekwe AM, Rodriguez NG, Quiroz KL, Mujica AP, Osmon K. 2019. Shiga toxin-producing *Escherichia coli* in mastitis: an international perspective. Foodborne Pathog Dis 16:229–243. https://doi.org/10.1089/fpd.2018.2491.
7. Schwengers O, Hoek A, Fritzenwanker M, Falgenhauer L, Hain T, Chakraborty T, Goesmann A. 2020. ASA^{3}P: an automatic and scalable pipeline for the assembly, annotation and higher-level analysis of closely related bacterial isolates. PLoS Comput Biol 16:e1007134. https://doi.org/10.1371/journal.pcbi.1007134.
8. Prjibelski A, Antipov D, Meleshko D, Lapidus A, Korobeynikov A. 2020. Using SPAdes de novo assembler. Curr Protoc Bioinformatics 70:e102. https://doi.org/10.1002/cpbi.102.
9. Tatusova T, DiCuccio M, Badretdin A, Chetvernin V, Nawrocki EP, Zaslavsky L, Lomsadze A, Pruitt KD, Borodovsky M, Ostell J. 2016. NCBI Prokaryotic Genome Annotation Pipeline. Nucleic Acids Res 44:6614–6624. https://doi.org/10.1093/nar/gkw569.
10. Bortolaia V, Kaas RS, Ruppe E, Roberts MC, Schwarz S, Cattoir V, Philippon A, Allesoe RL, Rebelo AR, Florensa AF, Falgenhauer L, Chakraborty T, Neumann B, Werner G, Bender JK, Stingl K, Nguyen M, Coppens J, Xavier BB, Malhotra-Kumar S, Westh H, Pinholt M, Anjum MF, Duggett NA, Kempf I, Nykäsenoja S, Olkkola S, Wieczorek K, Amaro A, Clemente L, Mossong J, Losch S, Ragimbeau C, Lund O, Aarestrup FM. 2020. ResFinder 4.0 for predictions of phenotypes from genotypes. J Antimicrob Chemother 75:3491–3500. https://doi.org/10.1093/jac/dkaa345.
11. Jolley KA, Bray JE, Maiden MCJ. 2018. Open-access bacterial population genomics: BIGSdb software, the PubMLST.org website and their applications. Wellcome Open Res 3:124. https://doi.org/10.12688/wellcomeopenres.14826.1.
12. Wirth T, Falush D, Lan R, Colles F, Mensa P, Wieler LH, Karch H, Reeves PR, Maiden MC, Ochman H, Achtman M. 2006. Sex and virulence in *Escherichia coli*: an evolutionary perspective. Mol Microbiol 60:1136–1151. https://doi.org/10.1111/j.1365-2958.2006.05172.x.
13. Jung D, Park S, Ruffini J, Dussault F, Dufour S, Ronholm J. 2021. Comparative genomic analysis of *Escherichia coli* isolates from cases of bovine clinical mastitis identifies nine specific pathotype marker genes. Microb Genom 7:e000597. https://doi.org/10.1099/mgen.0.000597.

Molecular Diversity
https://doi.org/10.1007/s11030-023-10731-6

ORIGINAL ARTICLE

WGS-based screening of the co-chaperone protein DjlA-induced curved DNA binding protein A (CbpA) from a new multidrug-resistant zoonotic mastitis-causing *Klebsiella pneumoniae* strain: a novel molecular target of selective flavonoids

Mohammad Habibur Rahman[1] · Salauddin Al Azad[2,12] · Mohammad Fahim Uddin[3,12] · Maisha Farzana[4] · Iffat Ara Sharmeen[5] · Kaifi Sultana Kabbo[6] · Anika Jabin[6,12] · Ashfaque Rahman[6,12] · Farhan Jamil[7] · Sanjida Ahmed Srishti[8] · Fahmida Haque Riya[8] · Towhid Khan[9] · Rasel Ahmed[10] · Nurunnahar[11] · Samiur Rahman[6,12] · Mohammad Ferdousur Rahman Khan[1] · Md. Bahanur Rahman[1]

Received: 22 June 2023 / Accepted: 11 September 2023

Abstract

The research aimed to establish a multidrug-resistant *Klebsiella pneumoniae*-induced genetic model for mastitis considering the alternative mechanisms of the DjlA-mediated CbpA protein regulation. The Whole Genome Sequencing of the newly isolated *K. pneumoniae* strain was conducted to annotate the frequently occurring antibiotic resistance and virulence factors following PCR and MALDI-TOF mass-spectrophotometry. Co-chaperon DjlA was identified and extracted via restriction digestion on PAGE. Based on the molecular string property analysis of different DnaJ and DnaK type genes, CbpA was identified to be regulated most by the DjlA protein during mastitis. Based on the quantum tunnel-cluster profiles, CbpA was modeled as a novel target for diversified biosynthetic, and chemosynthetic compounds. Pharmacokinetic and pharmacodynamic analyses were conducted to determine the maximal point-specificity of selective flavonoids in complexing with the CbpA macromolecule at molecular docking. The molecular dynamic simulation (100 ns) of each of the flavonoid-protein complexes was studied regarding the parameters RMSD, RMSF, Rg, SASA, MMGBSA, and intramolecular hydrogen bonds; where all of them resulted significantly. To ratify all the molecular dynamic simulation outputs, the potential stability of the flavonoids in complexing with CbpA can be remarked as Quercetin > Biochanin A > Kaempherol > Myricetin, which were all significant in comparison to the control Galangin. Finally, a comprehensive drug-gene interaction pathway for each of the flavonoids was developed to determine the simultaneous and quantitative-synergistic effects of different operons belonging to the DnaJ-type proteins on the metabolism of the tested pharmacophores in CbpA. Considering all the in vitro and in silico

✉ Md. Bahanur Rahman
bahanurr@bau.edu.bd

1 Molecular Microbiology and Vaccinology Lab, Department of Microbiology and Hygiene, Bangladesh Agricultural University, Mymensingh 2202, Bangladesh

2 Key Laboratory of Industrial Biotechnology, Ministry of Education, School of Biotechnology, Jiangnan University, Wuxi 214122, Jiangsu, People's Republic of China

3 College of Material Science and Engineering, Zhejiang Sci-Tech University, Hangzhou 310018, Zhejiang, People's Republic of China

4 School of Medicine, Dentistry and Nursing, University of Glasgow, University Avenue, Glasgow G12 8QQ, UK

5 Department of Mathematics & Natural Sciences, School of Data Sciences, BRAC University, Dhaka 1212, Bangladesh

6 Department of Biochemistry and Microbiology, North South University, Dhaka 1229, Bangladesh

7 Department of Pharmacy, University of Asia Pacific, Farmgate, Dhaka 1205, Bangladesh

8 School of Pharmacy, BRAC University, 66 Mohakhali, Dhaka 1212, Bangladesh

9 Department of Medicine, Comilla Medical College, Kuchaitoli, Comilla 3500, Bangladesh

10 School of Computing, Engineering and Digital Technologies, Teesside University, Middlesbrough TS1 3BX, UK

11 Department of Mathematics, Mawlana Bhashani Science and Technology University, Tangail 1902, Bangladesh

12 Immunoinformatics and Vaccinomics Research Unit, RPG Interface Lab, Jashore 7400, Bangladesh

Published online: 30 October 2023

parameters, DjlA-mediated CbpA can be a novel target for the tested flavonoids as the potential therapeutics of mastitis as futuristic drugs.

Graphical abstract

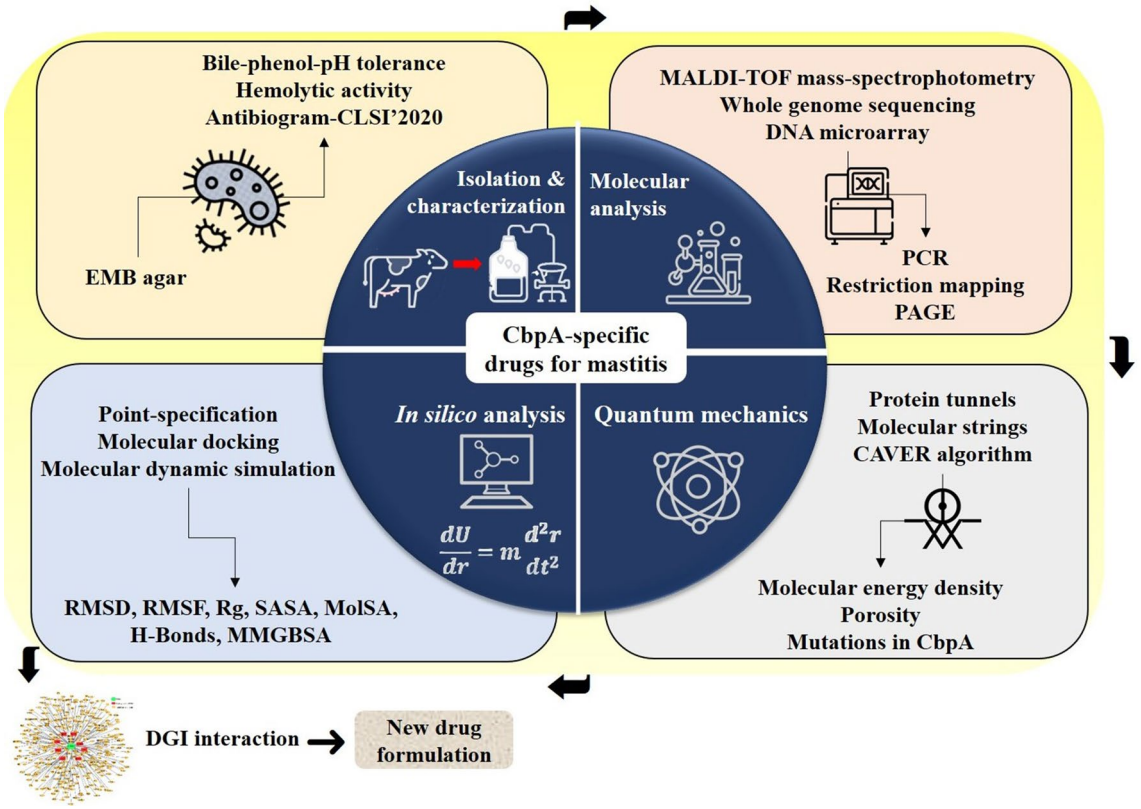

Keywords Whole genome sequencing · Multidrug-resistant *K. pneumoniae* · Co-chaperone DjlA protein · DnaK Co-chaperone CbpA protein · Pharmacokinetics and pharmacodynamics of natural flavonoids

Abbreviations

CFP	Cefoperazone
LZ	Linezolid
PNG	Penicillin G
CFT	Ceftaroline fosamil
DC	Doxycycline
SMA-TMP	Sulfamethoxazole and trimethoprim
TC	Tetracycline
CFS	Cefatrizine
CZD	Ceftazidime
CTA	Cefotaxime
IPN	Imipenem
MTC	Methicillin
GGI	Gene–gene interaction
PPI	Protein–protein interaction
WGS	Whole genome sequencing
ESBL	Extended-spectrum beta-lactamase
RMSD	Root mean square deviation
RMSF	Root mean square fluctuation
Rg	Radius of gyration
SASA	Solvent-accessible surface area
MolSA	Molecular surface area
MDS	Molecular dynamic simulation
CbpA	Curved DNA binding protein A
DGI	Drug-gene interaction
DPI	Drug-protein interaction

Introduction

Klebsiella pneumoniae has been recognized and distinguished as an infectious pathogenic agent and a potential threat to public health worldwide [1]. *K. pneumoniae* is a notable opportunistic pathogen, a natural inhabitant of the environment and mucosal surfaces of mammals and the human gastrointestinal tract [2]. It is typically a rod-shaped,

non-motile, encapsulated, facultative anaerobic bacterium belonging to the *Enterobacteriaceae* family [3]. Despite its natural presence in the normal flora of healthy humans and animals' skin, mouth, and intestine, this Gram-negative bacterium can develop various diseases, including pneumonia, respiratory tract infections, urinary tract infections (UTI), sepsis, meningitis, and infections at the surgical site in immunocompromised or healthcare-exposed patients, elderly, and neonates [4, 5]. The prevalence of *K. pneumoniae* infection is primarily found in nosocomial infections, with an annual global percentage rate of around 10% [6]. The two most recent predominant strains of *K. pneumoniae* are classic (cKp) and hypervirulent (hvKp) [1]. The multidrug-resistant (MDR) strains are more likely to appear from classic *K. pneumoniae* (cKp), which is characterized by low virulence, appearing primarily in healthcare settings as witnessed in Europe but carrying antimicrobial resistance genes (ARGs) [7]. Hypervirulent strains (hvKp) primarily cause community-acquired infections among healthy individuals via virulence genes. The pathogenesis of *K. pneumoniae* depends on the abilities of its virulence factors- pili, capsule, lipopolysaccharide (LPS), and iron–acquiring siderophore to bypass the host immune system. Type 1 and 3 pili promote adhesion to host cells and abiotic surfaces. hvKp exhibits capsular serotypes of K1 and K2 mainly, while classical Kp (cKp) has a significant percentage of K20 serotypes [8]. hvKp tends to produce more siderophore than cKp. However, the ones most specific to hvKp virulence and survival are aerobactin and salmochelin [9], while yersiniabactin may be acquired via horizontal gene transfer.

Antibiotic resistance rates in *K. pneumoniae* have been continuously increasing throughout the years. According to studies, third-generation cephalosporin, aminoglycosides, fluoroquinolones, and carbapenems have a non-susceptible rate for *K. pneumoniae* [10]. Whole genome sequencing (WGS) of cKp and hvKp strains dictates that both can get involved in co-integrated transfers [11]. Therefore, clinicians are concerned as several countries have already reported the emergence of multidrug-resistant, hypervirulent strains [12], which stemmed from the convergence of cKp and hvKp strains [13]. The hvKp contains virulent genes in its outer membrane vesicles (OMV), allowing horizontal transfer to extended-spectrum beta-lactamase (ESBL)-producing cKp (classic) [14]. Moreover, among CRKP isolates, sequence type ST11 co-carrying bla NDM-5 and bla KPC-2 genes were reported in more than half of its (ST11) percentage [15]. A chaperone ushers pili system (KPI) supports CRKP (ST-15) to make biofilms and adhere to various tissues [16].

Amidst the rising antibiotic resistance, it has been shown that some phytochemicals have antimicrobial efficacy against *K. pneumoniae*, inhibiting its growth of *K. pneumoniae* [17]. Some known chemical compounds, e.g., Limonene, Benzaldehyde, Acetophenone, Farnesene, Durenol, Thymol, Linalool, are mainly found in plant essential oils responsible for the inhibition of the growth of *K. pneumoniae*, which requires protein folding during environmental stress [18]. Chaperone proteins such as DnaK are highly conserved ATP-dependent proteins that play a crucial role in protein folding, including fixing misfolded or unfolded polypeptides that may arise during bacterial stress, heat shock, or pathogenic conditions [19]. Since they are upregulated in stressful conditions for cell survival, inhibition of their activity can lead to bacterial death [20]. Among the six co-chaperones of the DnaJ/Hsp40 family identified in *E.coli*, only three co-chaperones- DnaJ, CbpA, and DjlA can bind to DnaK [18]. The co-chaperone complex acts as a molecular switch that regulates chaperone proteins' activity, such as DnaK [21]. Therefore, particular plant-based flavonoids can target these conserved sequences of CbpA-CbpM protein complexes and CbpA-mediated DjlA protein functions, thus preventing their infection formation. In recent studies, in silico analysis has been emphasized in determining the target-specificity of the natural flavonoids as the potential antimicrobial drugs caused by *K. pneumoniae* [22].

Considering the aforementioned facts, the current study aimed to determine the whole genome sequencing of a multidrug-resistant *Klebsiella pneumoniae* strain to annotate the genes responsible for antibiotic resistance and virulence for mastitis infection. Besides, the DjlA-reinforced CbpA gene was identified as responsible for coding the CbpA chaperon protein which can induce mastitis formation. Finally, the DjlA-induced CbpA protein was established as a novel therapeutic target for selective natural flavonoids depending on their pharmacokinetic and pharmacodynamic profiles, while the involvement of a group of operons in metabolizing the pharmacophores was also analyzed comprehensively establishing drug-gene interaction (DGI) pathways.

Materials and methods

Sample collection

The milk samples were collected aseptically in separate falcon tubes (15 mL each) from 278 mastitis-infected cows after on-farm California Mastitis Test (CMT) from different farms of Chittagong, Dhaka, Gzipur, Jashore, Mymensingh, Pabna, Sirajganj and Sylhet districts of Bangladesh. Briefly, the udders of the cow were washed with clean water and allowed to dry; then, rub the udder teats with 70% ethanol; the first two strings of milk were discarded, and CMT was performed. The mastitis-positive milk samples were collected in separate sterilized falcon tubes preserved in the icebox and transported to Molecular Microbiology Lab., BAU, Mymensingh. The collected milk samples were processed for somatic cell count using LACTOSCAN COMBO's SCC

(Milkotronic Ltd, Bulgaria) according to the manufacturer's protocol [23]. The milk was mixed well with Sofia-Green dye, loaded into LACTOCHIP micro-fluidic camera, and computed based on the principles of the fluorescent microscope technique. Finally, data were recorded [24].

Isolation and biochemical characterization

The mastitis-infected milk (100 µL) was inoculated into 9.9 mL nutrient broth media and incubated at 37 °C (150 rpm). After 24 h of incubation, the consecutive cultures were streaked on different agar media and inoculated the plates at 37 °C for 18 h. Finally, the pure colonies were allowed to grow on EMB agar which is selective for *K. pneumoniae*. Isolation of single colonies from the pure culture, microscopic examination, and different biochemical tests like catalase, pH-bile-phenol tolerance tests [25, 26], and hemolysis [27].

Antibiogram profiling of the presumptive *K. pneumoniae*

The antibiogram profiling was completed by disk diffusion method on Mueller–Hinton Agar as per CLSI'2020. Briefly, the isolates were grown overnight in Tryptic soy broth (TSB) at 37 °C, 150 rpm, and inoculums were prepared (as 0.5 McFarland standard), set the antibiotic discs at equal distance on the plates and incubated at 37 °C for 18 h and measured the zone of inhibition diameter. Finally, the results were interpreted following the CLSI'2020 recommendation, where resistance, intermediate, and susceptibility indexes were individually and quantitatively assessed [28].

Molecular identification of the mastitis-causing *Klebsiella pneumoniae* strain

PCR and MALDI-TOF MS

DNA was extracted from the microbiologically suspected *K. pneumoniae* isolates and 16S rRNA gene PCR was performed. The PCR-confirmed isolates were allowed for MALDI-TOF MS (Matrix-assisted desorption ionization-time of flight mass spectrometry) detection using Bruker MALDI Biotyper following the manufacturer's protocols [29]. The evolutionary relationship of the isolated strain with its genetic neighbors was analyzed quantitatively using Phylogeny.fr [30].

Whole genome sequencing (WGS) of the identified *Klebsiella pneumoniae*

The PCR and MALDI-TOF MS confirmed *Klebsiella* spp. was allowed to WGS by "Illumina NextSeq 550". The WGS starts with DNA extraction (Genomic DNA Purification Kit A1120, Promega, USA) of the overnight growing bacterial culture, quantify (QuantiFluor® dsDNA System, Promega), and library prepared with Illumina DNA Prep. Then the library was quantified again, denatured, and diluted at 760 pMol to load into the system for sequencing. The sequences were assembled using the Unicycler pipeline (Galaxy Version 0.5.0 + galaxy1) [31] under the Galaxy server (https://usegalaxy.eu). The assembled files were submitted to NCBI GenBank to get new accession numbers for the identified strain [25].

Annotating the antibiotic resistance genes from the genome

In the current study, a wide range of antibiotic-resistant and virulent genes were classified to be present within the genomes of the microbial strains identified, considering their unique mechanisms. The antibiotic-resistance genes of the genome of the identified *Klebsiella* strain were profiled through CARD-RGI Interface [32, 33].

Profiling of the gene–gene interaction (GGI) networks behind the antibiotic resistance characteristics

The molecular string networks of the most sensitive antibiotic resistance and virulence genes were characterized using the STRING database [34]. The most viable genes were identified according to their ability to act as the interaction sources for the whole cluster strings at the time of infection initiation and progression in mastitis [35]. The interaction sources and signal recipients among the clusters were screened by Cytoscape 3.8.2 [36], which runs through the Java Runtime Environment interface [37].

Annotating the virulence factors from the genome

Likewise, the genes responsible for the microbial virulence properties were profiled using the VFDB Interface (http://www.mgc.ac.cn/VFs/main.htm) [38, 39]. The ontology of the virulent factors comprising genes with point-specific pathogenic functions to the multivalent-simultaneous and even non-defined functions were analyzed in this research. Both static and dynamic virulence gene profiles were compared to determine the most virulent factors among them [39]. Finally, the most virulent gene was identified from the annotated gene lists, encoding DjlA chaperone protein, which was isolated and screened through PCR, restriction digestion, and PAGE methods [26]. At the same time, the molecular string profile of the DjlA protein was also determined using Cytoscape 3.8.2 [34, 36]. The evolutionary

relationship of DjlA chaperone protein was characterized using NGPhylogeny.fr [40, 41].

CbpA-DjlA string analysis

A molecular string network between CbpA and DjlA was developed in STRING interface, and Cytoscape 3.8.2 [34, 36], where the strength of proteomic interactions was classified based on the number of their source of interactions among selective operon clusters. Besides, the group of proteins that help DjlA in provoking CbpA at the time of infection formation, was also identified [42].

In silico analysis of co-chaperone DjlA-induced CbpA protein as a therapeutic target

Protein optimization

The crystal structure of the CbpA was fetched from the Protein Data Bank (PDB) (PDB ID: 3UCS), as the target macromolecule of this study [43]. The follow-up protein optimization was conducted on "UCSF Chimera Software version-1.14" where the "A chain" of the protein was selected, followed by the removal of non-standard amino acids, atoms, water molecules, metal ions, and ligands [44, 45].

Quantum tunnel property analysis

After necessary optimization, the structure was conserved as "pdb format" for further docking analysis. For the active site prediction on the A chain, the pdb file was uploaded to the COACH-D algorithm [44, 46]. The "A chain protein homology model" was obtained by evaluating amino acid residues' binding energy and association. A total of five sites were obtained from the algorithm, among which the one with the highest binding affinity and the number of amino acid residues was selected for the quantum tunneling. The quantum tunneling of the "A chain" of 3UCS was done using the 'CAVER Algorithm' to elucidate its morphological features to predict the best active site for ligand docking [34, 36]. Based on the tunneling parameters, such as the protein tunnel length (Å), curvature (Radius), and bottleneck (Radius), tunnel cluster-2 the supramolecular docking region was verified [46].

Preparation of flavonoids

A total of five chemical compounds: Galangin (control), Kaempferol, Biochanin A, Myricetin, and Quercetin, were selected from the 200 compound library after their extensive Pharmacokinetic and QSAR properties. The 3D crystal structures of these phytochemicals were obtained from the PubChem database and conserved in "SDF" format [47]. The energy minimization was completed by UCSF Chimera 1.14, then transforming the structure to "mol2" format to perform molecular docking [37].

Molecular docking

Molecular super docking of each optimized ligand on the best binding site of the "CbpA-A chain" was conducted through the PyRx 0.8 software package [45, 47]. The macromolecule DjlA (PDB ID-3UCS) and each ligand complex were converted to the "pdbqt" file format on this software. After docking, the root means square deviation RMSD (Å) was analyzed, and binding affinities of each ligand–protein complex were filed up in ".csv file" format for further visualization. The ligand–protein complex was visualized on PyMOL (version 2.4.1) [43, 44], and each complex was converted into "pdb" format for post-docking analysis.

Post-docking analysis

After the qualitative assessment and visualization on PyMOL software, each ligand–protein complex underwent quantitative analysis of H-bonds and Hydrophobic interactions on LigPlot + (version 2.2) [46, 47], a JAVA runtime-based software [44, 45].

MDS analysis

The ligand-free protein's initial MDS was run on CABS-flex 2.0 for 10 ns. After observing the protein's natural structural modification in water, each of the ligand–protein complexes was run through LARMD for 3.1 ns to analyze principal component analysis (PCA), RMSD, root mean square fluctuation (RMSF), solvent accessible surface area (SASA) and MM-GBSA dG-binding score [34]. A final comprehensive MDS analysis of each of the ligand–protein complexes was conducted by GROMACS molecular dynamics package (version 5.1.2) for 100 ns to analyze RMSD, RMSF, SASA, Polar Surface Area (PSA), Radius of gyration (Rg), Ligand H-bonds, MMGBSA-dG binding score, and intramolecular H-bonds [36, 44]. The grid box size dimension was fixed to 10:10:10, with neutralizing ions (Na +) as the nullifying agent. The probe radius was 1.4 Å for SASA and molecular surface area (MolSA) analysis [43, 47]. All the results obtained from the simulation were transferred and conserved in ".csv file" format.

Drug-gene interaction (DGI) analysis

The individual effects of each of the tested flavonoid pharmacophores on a group of gene clusters based on their DGI properties were analyzed using STITCH, GeneMANIA, and

Cytoscape 3.8.2 combinedly [34, 36]. In that case, the synergistic and simultaneous impacts of the operons (groups of genes with similar functions) on the individual flavonoids were considered [34].

Statistical analysis and graphical representation

The statistical analysis and graphical representation were prepared using the 'GraphPad Prism version 8.0.1' software package (for Mac OS) [48–51]; and the 'R programming' (version R-4.0.2 for Linux) [40, 52, 53].

Results

Isolation, identification, and characterization

The isolated pathogen was identified as *K. pneumoniae* strain BR-MHR521 (NCBI BioProject Accession No. PRJNA915214) based on the whole genome mapping. The newly identified strain showed tolerance to the pH 5.5; 1.0% bile salt; 0.3% phenol; gram-negative; non-motile; catalase positive; oxidase negative; and indole test negative.

Antibiogram of *K. pneumoniae* strain BR-MHR521

The isolated *K. pneumoniae* (BR-MHR521) showed different susceptibility to different antibiotics in the disk diffusion method. The antibiogram (Fig. 1) shows that *K. pneumoniae* is highly susceptible to Cefoperazone (CFP), Linezolid (LZ), and Penicillin G (PNG). Moreover, the antibiogram shows that *K. pneumoniae* is moderately susceptible to ceftaroline fosamil (CFT), Doxycycline (DC), sulfamethoxazole and trimethoprim (SMA-TMP), and Tetracycline (TC); additionally, resistant to antibiotics, including Cefatrizine (CFS), ceftazidime (CZD), Cefotaxime (CTA), Imipenem (IPN), and methicillin (MTC).

Annotating the antibiotic resistance genes

The current study resulted that most of the genes for promoting antibiotic resistance in *K. pneumoniae* means-MarA (STRING Identifier: JG24_11650); BaeR (STRING Identifier: JG24_17005); and RsmA (STRING Identifier: GCA_001598715_02965) can play pivotal roles as interaction source for the neighboring genes amid their individual gene–gene-interaction (GGI) network except the CRP gene (STRING Identifier: JG24_26820) which mainly act as the interaction recipient from the other gene clusters of its genetic string network (Fig. 2). Among the frequent resistance genes, MarA roles as the interaction source of seven other antibiotic resistance-provoking genes, including AdaA (JG24_28085), AraC (JG24_13785), MarR (JG24_11655), Marc (JG24_11665), AraC (JG24_13135), AraC (JG24_22430), RhaR (JG24_26050) genes responsible for differential transcriptional modulation at resistance formation (Fig. 2A). In contrast, the CRP gene maintains the gene–gene-interaction (GGI) as an interaction signal receiver from seven different transcription-regulating genes, such as RpoA, RpoB, RpoD, RpoZ, and GltB genes (Fig. 2B). Besides, the BaeR gene provides an interaction signal to the CreC (JG24_29395), ArcB (JG24_22980), BarA (JG24_20205), and hybrid sensory histidine kinase (JG24_22255) genes (Fig. 2C). The RmsA gene signals to the similar-functioning LptD (GCA_001598715_02968), SurA (GCA_001598715_02967), RpsD (GCA_001598715_04304) genes of a string (Fig. 2D). Depending on the number of interaction signals, MarA is comparatively more vigorous than the rest holding the most antibiotic resistance mechanism in *K. pneumoniae*.

Annotating the virulence genes

The present study identified Aerobactin, RmpA, DjlA, and Colibactin coding genes as virulence factors. The DnaJ gene for DjlA biosynthesis resulted as the most significant one,

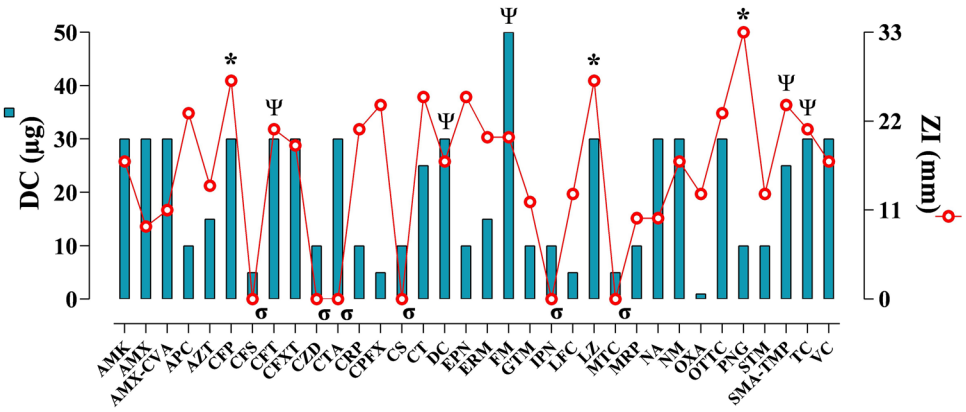

Fig. 1 Graphical illustration of the antibiotic sensitivity of *K. pneumoniae* (BR-MHR521) against 34 antibiotics based on the zone of inhibition (ZI) (mm) and dose concentration (DC) (µg)

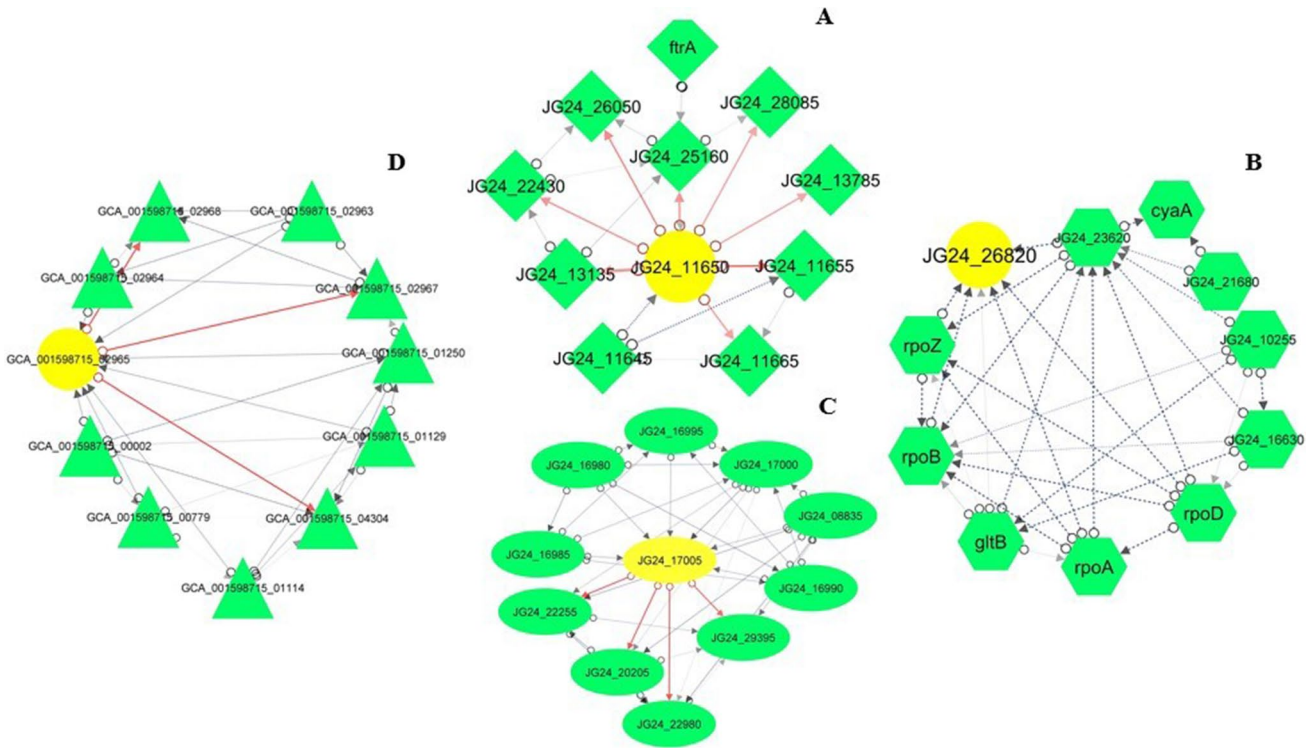

Fig. 2 Analysis of the molecular networks of the most prominent antibiotic resistance genes means MarA (yellow circle and green diamond) (**A**); CRP (yellow circle and blue hexagon) (**B**); BaeR (yellow circle and blue circle) (**C**); and RsmA (yellow circle and green triangle) (**D**), where each of them represents their strings accordingly

considering the mechanism of infection formation at selective anomalies.

Identification of chaperone DnaJ gene

The DnaJ gene encoding "DjlA chaperon protein," especially the "heat shock protein," was preliminary identified through restriction digestion and PAGE with a length of 1104 bp studying the position of the gene inside the whole genome, which was most similar to the sequence of *K. pneumoniae* subsp. pneumoniae HS11286 chromosome (Gene Bank Accession No. NC016845.1) studied previously (Fig. 3A).

DjlA-mediated protein–protein interaction (PPI) involved in CbpA regulation

DjlA protein is interconnected with a group of differential chaperone proteins means SurA, DnaK, GrpE, NfuA, HscA, NifU, and JG24_16675 (nitrogen fixation protein NifU coding) genes in the molecular strings (Fig. 3). Besides, a few functionally non-defined proteins were found within the molecular string networks of DjlA, such as IptD and JG24_01530 proteins (Fig. 3B). Considering the identified PPI profile, DjlA acts as the interaction recipient of all the aforementioned protein signals, including the functionally non-defined ones, staying at the center of the string mesh (Fig. 3B). A quantitative interaction strength among these proteins were identified based on molecular-string scores, where CbpA was found to be vigorously connected with the DjlA at all standards (Fig. 3C). According to the molecular STRING profiles of *K. pneumoniae*, proteins like DnaK, GrpE, and HscA from DjlA protein cluster, can directly regulate the functions of CbpA from the time of onset to severe progression of infection, resulted in this research.

The evolutionary relationship study for DjlA

The phylogenetic analysis of DjlA chaperone protein (NCBI GI: 496082963; Accession: WP_008807470.1) revealed that it possesses a very significant evolutionary relationship with a group of chaperone proteins (Fig. 4A) from different microorganisms, including- WP_110233507.1 from *Klebsiella variicola*; WP_243234166.1, WP_225371030.1, HBU8762037.1, and CAF2004784.1 from *K. pneumoniae* considering both the radial (Fig. 4B) and linear forms (Fig. 4C) of analysis. In all the cases, the genetic similarity and evolutionary matching score of DjlA chaperone protein with the other chaperones were $p < 0.01$ on a scale $\alpha = 0.05$ means very significant.

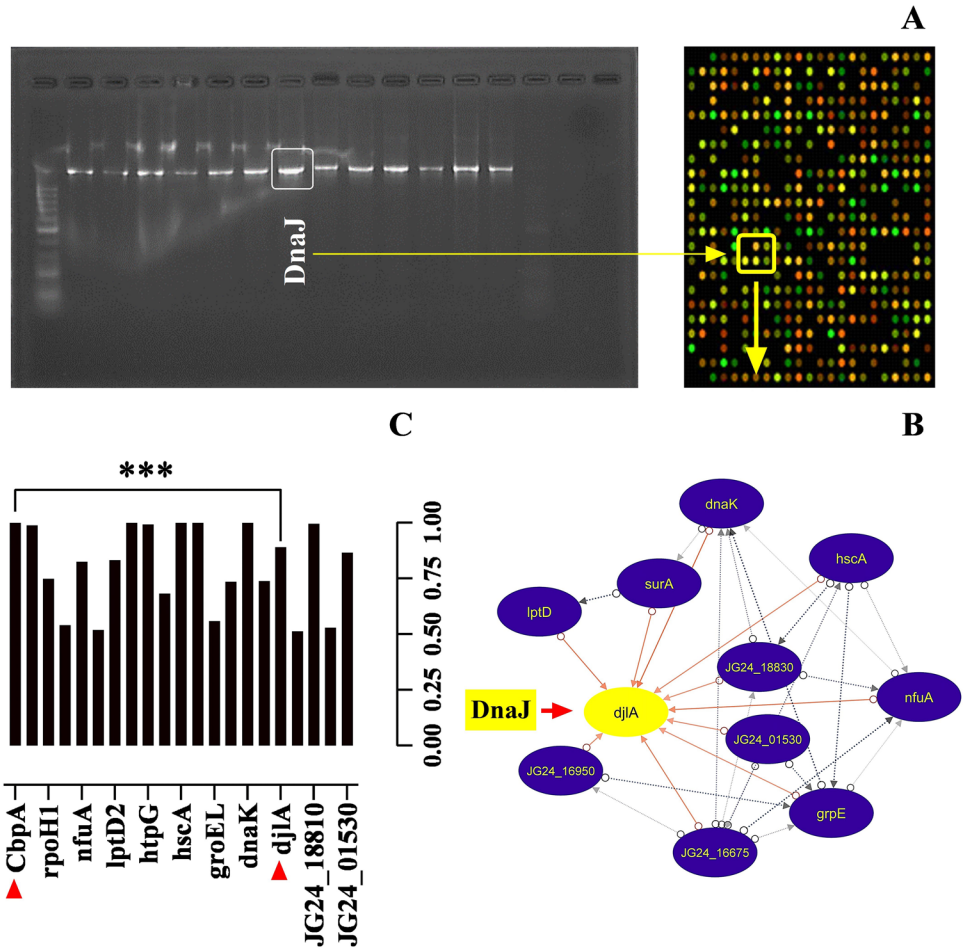

Fig. 3 Polyacrylamide Gel Electrophoresis of DjlA gene encoding DjlA protein extracted from K. pneumoniae strain BR-MHR521. The red arrows toward DjlA indicate the interaction sources of DjlA inside the PPI strings

Pharmacokinetic profiling

The values of Log P of the five ligands ranged from 1.69 to 2.87, where Biochanin A harbored the highest value comparatively. The blood–brain-barrier values of Myricetin were the lowest (− 1.493), whereas Biochanin A showed BBB permeability (− 0.221). There was no violence regarding Lipinski's rules in any ligands except for the test ligand Myricetin (Table 1). Among the test ligands, Biochanin A resulted in maximum intestinal absorption (93.028%). All five compounds' total clearance (TC) values were positive and ranged between 0.256 and 0.477. None of the ligands showed any hepatotoxicity or AMES toxicity (AT). Also, the LD50 level of Myricetin was the highest (2.49) among all the ligands. All five ligands, including the control, showed significant maximum-tolerated doses (MTD), maintaining the range of 0.33 to 0.736 log mg/kg/day (Table 1). The QSAR profile indicates substantial antibacterial activities for all the ligands. Biochanin A and the control ligand Galangin showed antiviral effects (Table 2).

Quantum tunneling of CbpA

Quantum tunnel profiling reveals a total of two tunnels each containing seven sub-tunnels, having a distinct length, curvature, and bottleneck radius. Sub-tunnels of cluster 2 have bottleneck radius (BR) ranging from 1.02 Å, 1.93 Å, and a length of 9.56 Å (Fig. 5A). Tunnel cluster 2 had length manifolds greater than cluster 1 sub-tunnels. However, cluster 2 fell short of a much narrower BR than cluster 1. The bottleneck point of tunnel cluster 2 contained seven amino acid residues-53Val, 53Ile, *2Me, 56A**, 55Arg, 74Leu, and 70Ile. As amino acid residues were more significant in the cluster 2 bottleneck region, the formation of H-bond and stable ligands have a much greater chance of docking inside those sub-tunnels (Fig. 5B).

The sub-tunnels of tunnel cluster-1 possessed a bottleneck radius (BR) between 2.3 Å, Curvature between 1.05 Å, and a length between 1.47 Å (Fig. 5A). Tunnel cluster 1 has a shorter length of manifolds than cluster 2. The bottleneck radius (BR) of tunnel cluster 1 was broader as the value ranges from 0 to 2.3 Å, higher than Cluster 2. The bottleneck

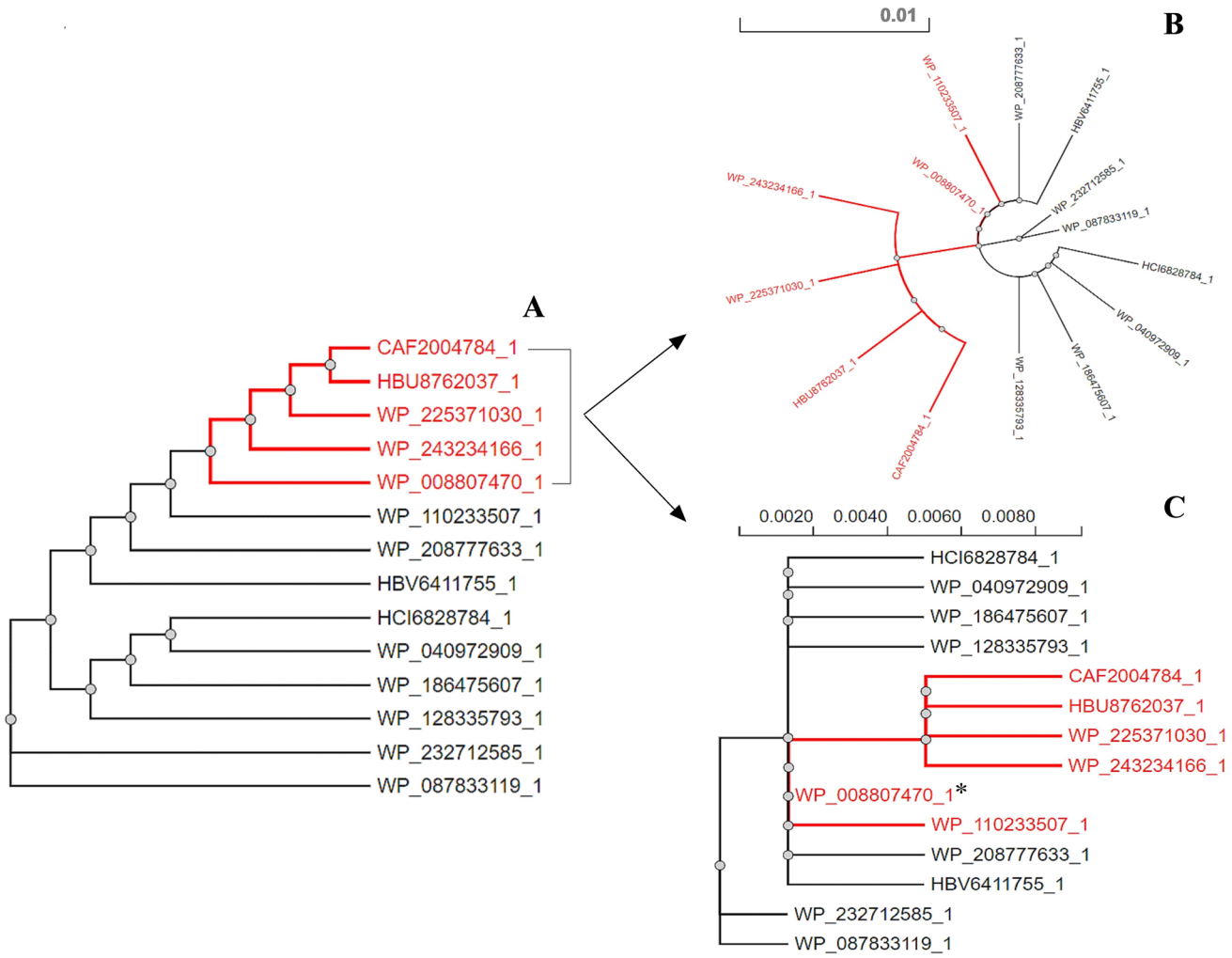

Fig. 4 The evolutionary relationship of co-chaperone protein Dj1A of *K. pneumoniae* along with the basic genetic similarity found on these six chaperone proteins (Red nodes) (**A**); the radial forms of the relationship with a score of 0.01 (**B**); and the phylogenic distances (**C**)

Table 1 Pharmacokinetics profiling of ADMET and QSAR for ligand validation

Ligands	CID	MoW	LogP	H-Ac	H-Do	NRB	BBB	NLV	DL	IA	TC	AT	LD50	HT	MTD
Galangin	5,281,616	270.24	2.57	5	3	1	− 0.748	0	Yes	93.985	0.256	No	2.45	No	0.33
Kaempherol	5,280,863	286.24	2.28	6	4	1	− 0.939	0	Yes	74.29	0.477	No	2.45	No	0.531
Biochanin A	5,280,373	284.26	2.87	5	2	2	− 0.221	0	Yes	93.028	0.247	No	1.85	No	0.4
Myricetin	5,281,672	318.23	1.69	8	6	1	− 1.493	1	Yes	65.93	0.422	No	2.49	No	0.51
Quercetin	5,280,343	302.23	1.98	7	5	1	− 1.098	0	Yes	77.207	0.407	No	2.47	No	0.49

QSAR quantitative structure–activity relationship, *ADMET* absorption, distribution, metabolism, excretion, and toxicity, *MoW* molecular weight, g/mol, *LogP* predicted octanol/water partition coefficient, *H-Ac* no. of hydrogen bond acceptor, *H-Do* no. of hydrogen bond donor, *NRB* no. of rotatable bonds, *BBB* blood brain barrier, *NLV* no. of Lipinski's rule violations, *DL* drug-likeness, *IA* intestinal absorption, % absorbed, *TC* total clearance, log ml/min/kg, *AT* AMES toxicity, *LD50* oral rat acute toxicity, *HT* hepatotoxicity, *MTD* maximum tolerated dose for human

point of tunnel cluster 1 contained amino acid residues, including 52 ILE, 32-MET, 31-GLY, and 33*E. The tunnel was found to be surrounded by amino acid residues as the ligand moved through that. So, there was comparatively less chance of super docking inside these sub-tunnels (Fig. 5C).

Molecular docking

The control ligand Galangin and the test ligand Biochanin A produced the lowest binding affinity scores of − 5.9 kcal/mol with the A chain of CbpA chaperone protein (Table 3). In

Table 2 QSAR-based bioactivity prediction for ligand validation

Compounds	Prediction of activity spectra for substances (*Pa* = 0.3 to 0.7)		
	Anti-infective	Antiviral	Anti-bacterial
Galangin (control)	✓	✓	✓
Kaempherol	✓	×	✓
Biochanin A	✓	✓	✓
Myricetin	✓	×	✓
Quercetin	✓	×	✓

contrast, the upper and lower RMSD values and the MMGBSA α-DG score were higher for Biochanin A. Myricetin harbored the highest binding affinity value (− 6.3 kcal/mol). However, it showed the lowest MMGBSA α-DG score (− 26.11) (Table 3). Quercetin showed the second-highest binding affinity of − 6.2 kcal/mol and the highest MMGBSA α-DG score of − 43.15. On the other hand, Kaempferol has a binding affinity of − 6.1 kcal/mol and α-DG score comparatively higher than Myricetin (Table 3).

Post-docking analysis

The control ligand Galangin has three stable hydrogen bonds from the same amino acid residue Arg96 when interacting with the CbpA (PDB: 3UCS) macromolecule. The atomic distance of these bonds has been measured as 3.03 Å, 3.10 Å, and 3.16 Å, while the number of hydrophobic interactions is four, namely from His100, Phe97, Leu94 and Arg93 residues (Fig. 6A). The Kaempferol-3UCS complex showed six hydrogen bonds, i.e., two stable bonds from each amino acid residue, such as Arg55 (3.02 Å, 2.82 Å), Ala71 (2.85 Å, 3.13 Å), Thr75 (2.70 Å, 2.92 Å). On the other hand, the kaempferol-3UCS complex shows five hydrophobic interactions with Gly31, Ile52, Glu34, Leu74, and Met32 (Fig. 6B). Biochanin A presented two hydrogen bonds from Arg55 (3.06 Å) and Gly31 (2.92 Å) and five hydrophobic interactions from Thr51, Arg58, Met32, Leu74, and Ile52 residues (Fig. 6C). In the case of Myricetin-3UCS complex, Arg55 (3.17 Å), Ala 71 (2.84 Å), Thr75 (3.15 Å, 2.90 Å), and Asp 78 (2.98 Å) are the five hydrogen bonds (Fig. 6D), whereas the hydrophobic residues present inside stem from Leu74, Ile52, Met32, and Thr51 residues (Table 4). Lastly, Quercetin forms four hydrogen bonds with the macromolecule that involve Arg55 (3.16 Å, 2.96 Å), Asp78 (2.69 Å), and Thr75 (3.04 Å). Quercetin also showed six hydrophobic interactions, namely Leu74, Ile52, Met32, Gly31, Ala71, and Val72 (Table 4). Considering the number of hydrophobic interactions, Quercetin has the nearest contiguity with six

Table 3 Molecular docking analysis of the targeted macromolecule CbpA with the tested flavonoids

Receptor	Ligands	Binding affinity (Kcal/mol)	RMSD (Å)		MMGBSA-DG
			UB (Å)	LB (Å)	
CbpA	Galangin	− 5.9	6.729	2.455	− 31.31
CbpA	Kaemph-erol	− 6.1	6.828	2.559	− 33.35
CbpA	Biochanin A	− 5.9	7.323	2.486	− 37.46
CbpA	Myricetin	− 6.3	7.275	2.671	− 26.11
CbpA	Quercetin	− 6.2	6.981	2.585	− 43.15

UB upper bounds, *LB* lower bounds

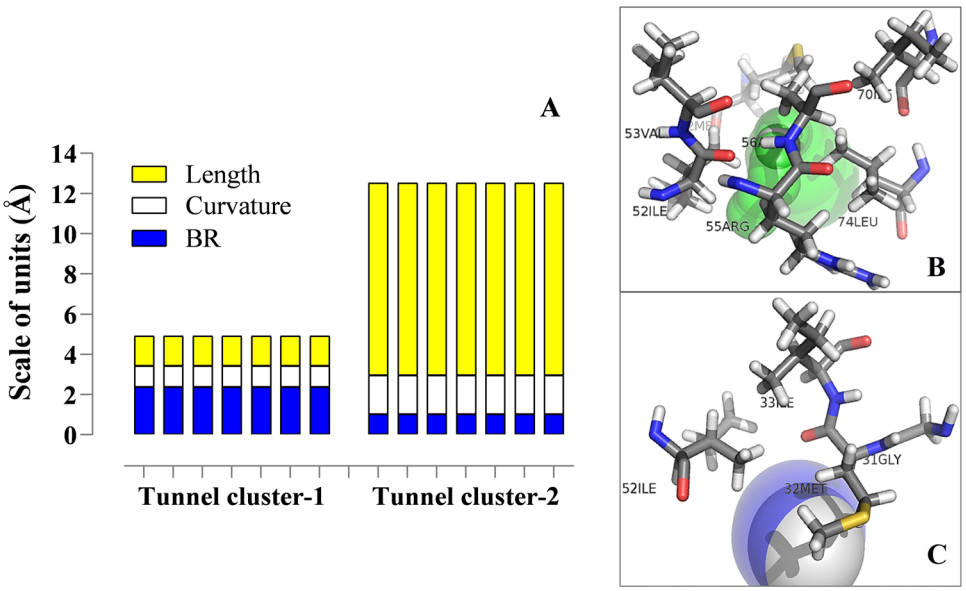

Fig. 5 Visualization of the quantum tunnels of the CbpA considering the tunnel length (Å) and bottleneck radius (Å), and curvature (Å) for assigning the tentative super docking position/s for ligands

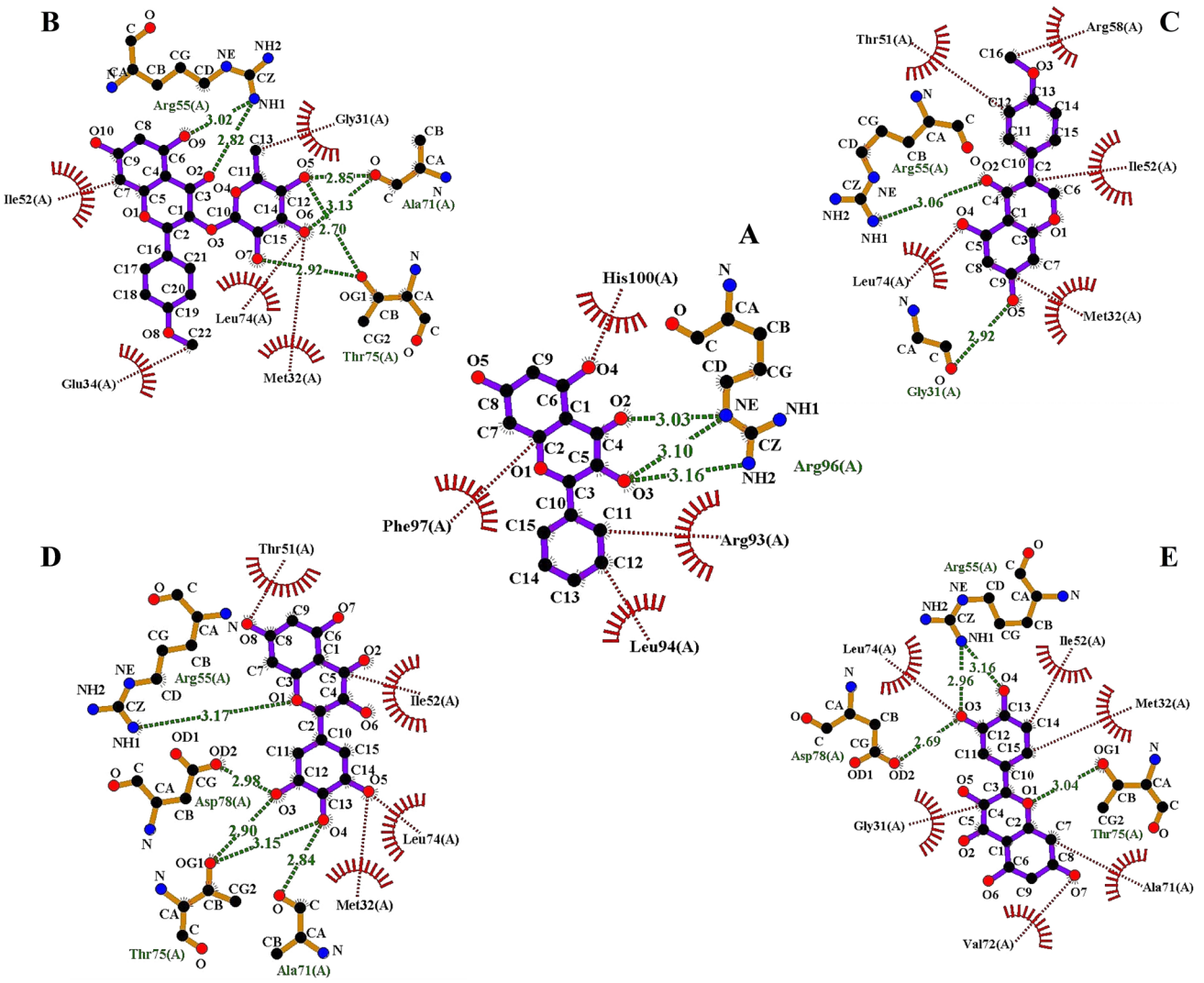

Fig. 6 Identification of the drug-protein interactions (DPI) considering their hydrogen bonds (green lines) and hydrophobic/non-covalent interactions (red lines). The atomic distances are calculated in Å. The CbpA protein is complexed with Galangin (control ligand) (**A**), Kaempferol (**B**), Biochanin A (**C**), Myricetin (**D**), and Quercetin (**E**)

Table 4 Analysis of the hydrogen bonding and noncovalent (hydrophobic) interactions between the ligand atoms of each of the ligands and the amino acid residues of 3UCS following the supramolecular docking

Macromolecule	Ligands	Point-specific amino acid interactions with the ligand atoms	
		Hydrogen bond interactions	Hydrophobic interactions
3UCS	Galangin (control)	Arg96 (3.03 Å, 3.10 Å, 3.16 Å)	His100, Phe97, Leu94, Arg93
3UCS	Kaempherol	Arg55 (3.02 Å, 2.82 Å), Ala71 (2.85 Å, 3.13 Å), Thr75 (2.70 Å, 2.92 Å)	Gly31, Ile52, Glu34, Leu74, Met32
3UCS	Biochanin A	Arg55 (3.06 Å), Gly31 (2.92 Å)	Thr51, Arg58, Met32, Leu74, Ile52
3UCS	Myricetin	Arg55 (3.17 Å), Ala 71 (2.84 Å), Thr75 (3.15 Å, 2.90 Å), Asp 78 (2.98 Å)	Leu74, Ile52, Met32, Thr51
3UCS	Quercetin	Arg55 (3.16 Å, 2.96 Å), Asp78 (2.69 Å), Thr75 (3.04 Å)	Leu74, Ile52, Met32, Gly31, Ala71, Val72

amino acids (Fig. 6E), the highest among all the ligands, and four hydrogen bonds.

MDS analysis (100 ns)

RMSD analysis

In the MDS analysis, the RMSD values ranged between 0.125 and 0.78 nm for the control ligand Galangin. In contrast, the ranges for the test ligands were 0.137 to 0.658 nm; 0.162 to 0.496 nm; 0.193 to 1.0 nm; and 0.104 to 0.639 nm for Kaempferol, Biochanin A, Myricetin, and Quercetin, respectively (Fig. 7A).

Rg analysis

The profile of the Radius of gyration (Rg) shows the labile nature of the protein. Myricetin showed a higher Rg profile, varying from 1.429 to 1.942 nm, indicating that the molecules are loosely packed. In contrast, the docked complex Biochanin A had lower Rg deviations between 1.74 and 2.045 nm. The control ligand, Galangin, appeared to have an Rg score between 1.527 and 1.877 nm. Besides, the test ligands Kaempferol and Quercetin exhibited Rg values ranging from 1.613 to 1.932 nm; 1.564 to 1.908 nm, respectively (Fig. 7B).

Intramolecular H-bonds

During the MDS analysis, the number of hydrogen bonds was counted for Galangin, Biochanin A, Kaempferol, Myricetin, and Quercetin (Fig. 7C) precursor for 100 ns. For the control ligand Galangin, the lowest number of hydrogen bonds was 62, and the highest was 90. For Biochanin A, the protein hydrogen bonds were between 60 and 87. The lowest number of hydrogen bonds for Kaempferol was 61 at 30.1 ns, and the highest number of hydrogen bonds formed at 48.1 ns which was 91 in number. Myricetin and Quercetin's lowest number of hydrogen bonds were 59 and formed at 3.8 and 23.3 ns, respectively. Myricetin formed 84 hydrogen bonds at 2.55 ns, and Quercetin formed a maximum of 90 hydrogen bonds at 2.45 ns.

The number of hydrogen bonds formed between the macromolecule and each of the targeted ligands Galangin, Biochanin A, Kaempherol, Myricetin, and Quercetin was also determined for the 100 ns of molecular dynamic simulation, the results of which are represented in Fig. 7D. For Biochanin A and Kaempherol, the highest number of hydrogen

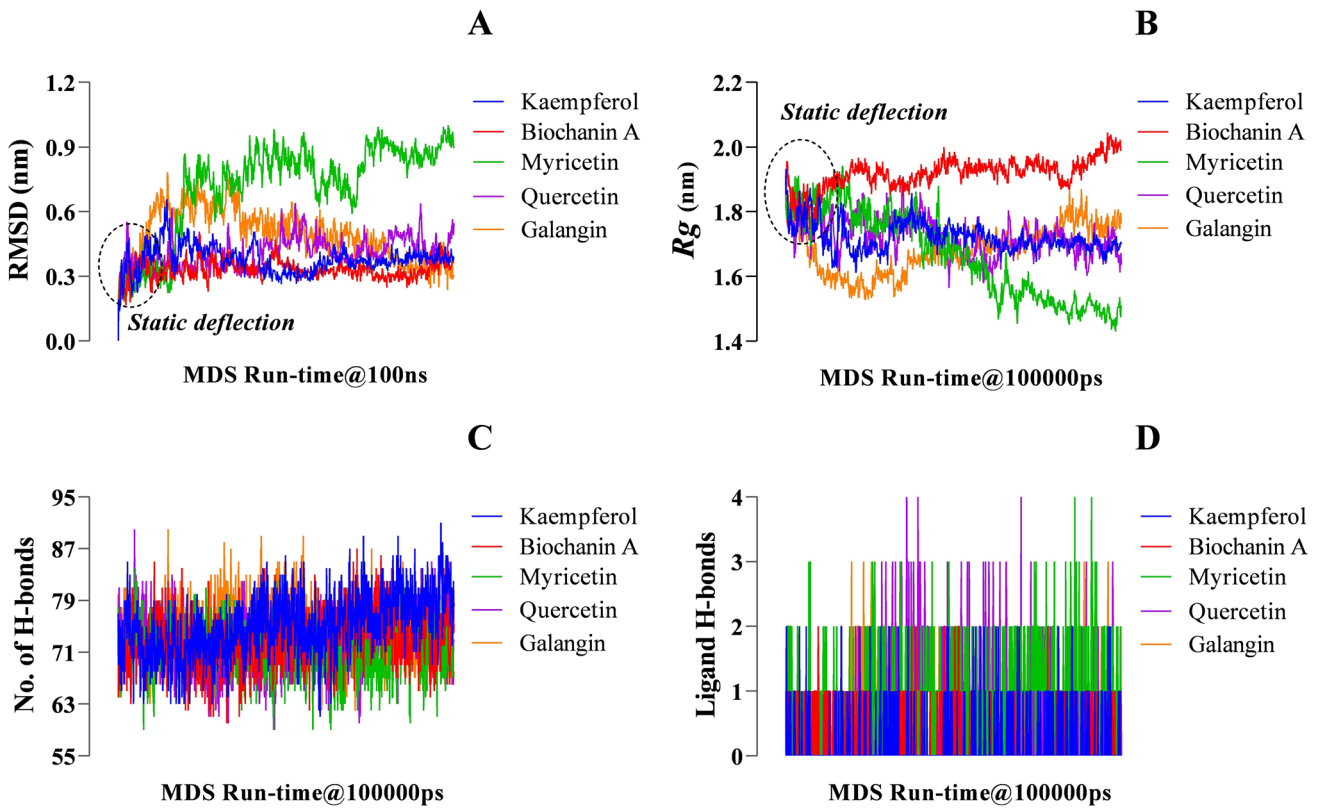

Fig. 7 Illustration of the molecular dynamics simulation results following 100 ns of runtime for each of the individual ligand-CbpA complexes, including RMSD (**A**), Rg (**B**), intramolecular H-bonds (**C**), and the ligand H-bonds (**D**)

bonds with these ligands was 2, and the lowest was 0. In the Galangin-CbpA complex, the highest number of ligand hydrogen bonds was 3, and the lowest was 0. The number of ligand hydrogen bonds was the same for Myricetin and Quercetin—the highest being four and the lowest being 0 with each ligand.

SASA analysis

The SASA analysis of the ligand–protein complex maintained at a water probe radius of 1.4 Å, the total area or polar and apolar energy 2553.07 and 4643.29 Å^2, respectively, for all of the five ligand–protein complexes (Table 5). SASA values of the ligand–protein complexes of Biochanin A-3UCS value 60.625–79.477 nm^2 is the highest value range of the five ligands. The Myricetin-CbpA complex ranged between 61.55 and 79.24 nm^2, the second-highest value, followed by the Quercetin-3UCS complex, which resulted between 59.83 and 77.575 nm^2; and the control Galangin with the lowest value range of 60.52–77.807 nm^2. Kaempherol-CbpA scored between 57.839 and 78.663 nm^2, which falls within Quercetin, Galangin, Myricetin, and Biochanin A (Fig. 8A).

RMSF analysis

Myricetin scored 1.2753 to 0.1792 nm followed by quercetin values scored 0.939 to 0.1175 nm as the two most significant ligands. Additionally, 0.5903 to 0.1322 nm; 0.9629 to 0.1323 nm; and 0.9179 to 0.1173 nm values were scored by Biochanin A, Galangin, and Kaempherol, respectively. Analysis of the RMSF values revealed significant differences in the protein complexes at a residue near the binding site (Fig. 8B).

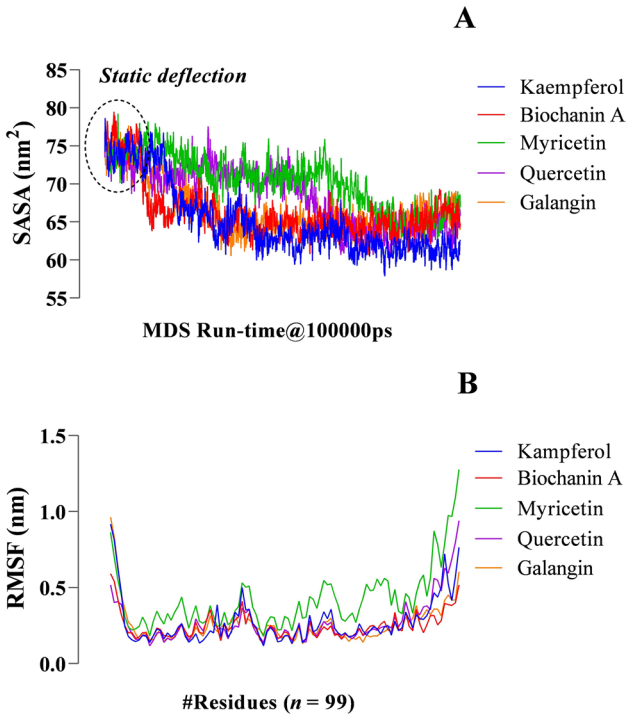

Fig. 8 Graphical representation of the SASA (**A**), and RMSF (**B**) scores resulting from the molecular dynamic simulation of 100 ns

DGI profiling of the tested flavonoids

The current research revealed that Quercetin strongly interacts with the CYP2C8, CYP2C18, CYP1A2, CYP3A4, CYP2E1, and CYP2C19 following its complexing with the CbpA protein (Fig. 9A). Similarly, Myricetin forms connectivity for its metabolism to CbpA through the ATK1, PPARG, NR1H3, SIRT1, and PIK3CG genes (Fig. 9B). Besides, CYP2E1, UGT1A5, UGT1A9, UGT1A7, UGT1A6, UGT1A8, UGT1A4, UGT1A3, UGT1A1, and UGT1A10 genes significantly influence the metabolism of Biochanin A (Fig. 9C). Surprisingly, the most viable and significant DGI was found to be established by Kaempferol, where UGT1A7, UGT1A2. UGT1A8, UGT1A6, UGT1A5, UGT1A3, UGT1A11, UGT1A1, UGT1A10, UGT1A4, UGT2B7, and UGT2B28 genes were involved (Fig. 9D). In contrast to the test ligands, Galangin impacts

Table 5 Solvent accessible surface area (Å^2) referring the area to energy ratio over the entire dynamic simulation process with polar and Apolar regions precisely

Macromolecule	Ligands	WPR (Å)	GIC	TNR	Total Area/Energy			NSA	NBA	NA with ASP
					Polar	Apolar	UNK			
3UCS	Biochanin A	1.4	No	99	2553.07	4643.29	0	503	286	174
3UCS	Galangin	1.4	No	99	2553.07	4643.29	0	503	286	174
3UCS	Kaempherol	1.4	No	99	2553.07	4643.29	0	503	286	174
3UCS	Myricetin	1.4	No	99	2553.07	4643.29	0	503	286	174
3UCS	Quercetin	1.4	No	99	2553.07	4643.29	0	503	286	174

WPR water probe radius, *GIC* gradient in calculation, *TNR* total no. of residues, *UNK* unknown, *NSA* number of surface atoms, *NBA* number of buried atoms, *NA with ASP* number of atoms with atomic solvation parameters

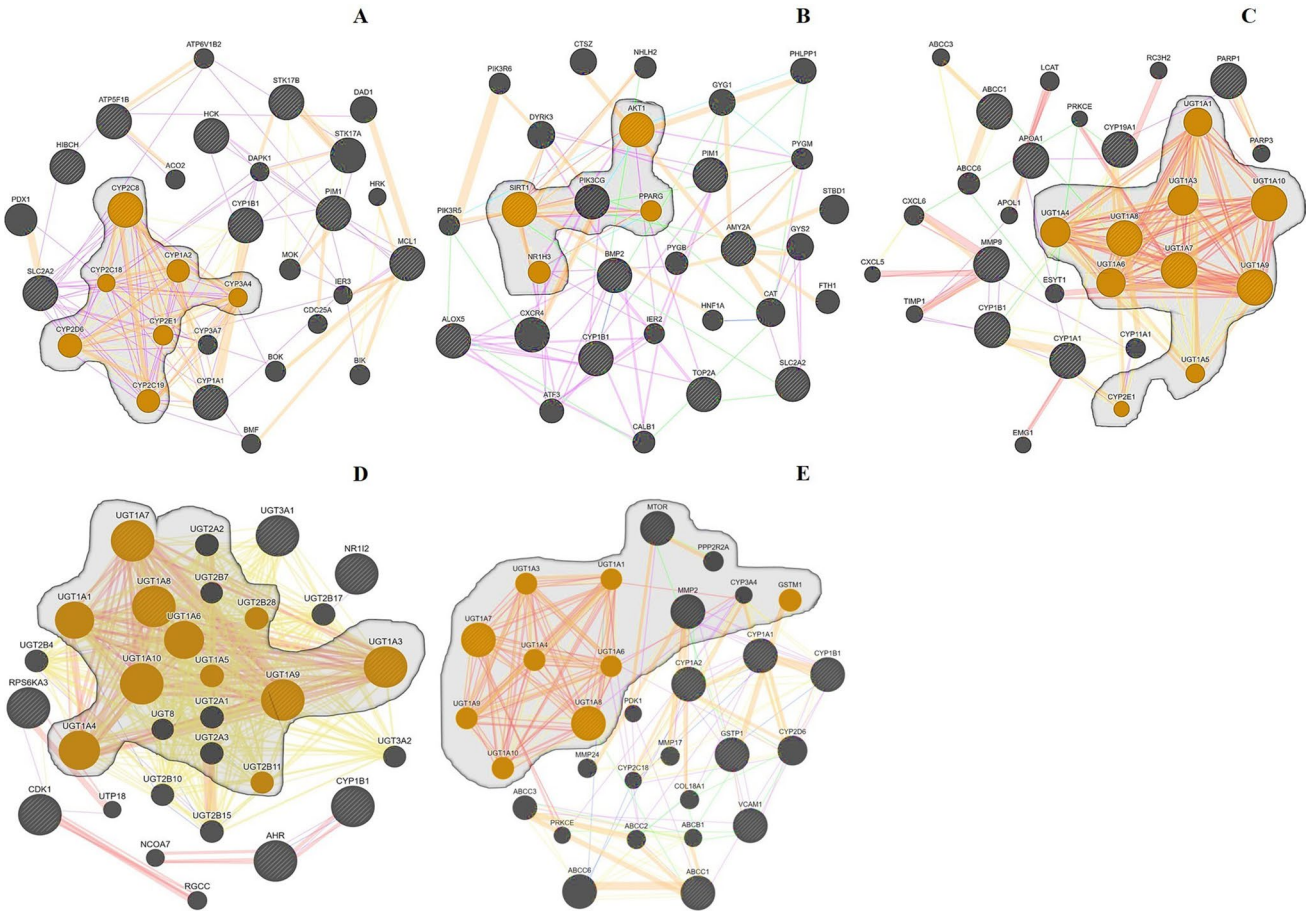

Fig. 9 Illustration of the DGI profiles of different groups of genes in metabolizing Quercetin (**A**); Myricetin (**B**); Biochanin A (**C**); Kaempferol (**D**); and the control drug Galangin (**E**). The most interactive genes for the particular drugs involved in metabolizing them on CbpA are confined within the gradient area

on the UGT1A3, UGT1A4, UGT1A7, UGT1A1, UGT1A9, UGT1A6, UGT1A8, UGT1A10, and GSTM1 (Fig. 9E).

Discussion

Isolation and characterization of morphological and biochemical properties

The *K. pneumoniae* strain BR-MHR521 (NCBI BioProject Accession No. PRJNA915214) exhibits good tolerance levels for various pH, bile, and phenol. Comparable results of this gram-negative pathogen were found for the morphological, physiological, and biochemical characteristics [54].

Antibiogram profiling of *K. pneumoniae*

The antibiotic susceptibility of the isolates was tested using the disk diffusion method against 34 panels of antibiotics to determine best its resistance potential, represented as an antibiogram in (Fig. 1) [55]. In this study, the isolated strain of *K. pneumoniae* was highly susceptible to Cefoperazone (CFP), Linezolid (LZ), and Penicillin G (PNG) and moderately susceptible to Ceftaroline Fosamil (CFT), Doxycycline (DC), Sulfamethoxazole and Trimethoprim (SMA-TMP), and Tetracycline (TC). Moreover, the KP isolates are also susceptible to other antibiotics, such as Chloramphenicol and Ciprofloxacin. A study revealed similar aligning results where they found out that Tetracycline and Ciprofloxacin were among the most potent antibiotics against *K. pneumoniae* [56]. On the other hand, strains of *K. pneumoniae* were found to be resistant to multiple antibiotics such as Cefatrizine (CFS), Ceftazidime (CZD), Cefotaxime (CTA), Imipenem (IPN), and Methicillin (MTC), Cefoxitin, Gentamicin, Levofloxacin, Oxacillin; with intermediate resistance to Azithromycin and Erythromycin (Fig. 1). Resistance of *K. pneumoniae* to antibiotics belonging to the cephalosporin family (except for cephamycins Cefoxitin and Cefotetan), such as CZD in our study, has also been reported previously [57].

Genetic interaction network among antibiotic-resistant genes

The current study produced a STRING network among prominent antibiotic-resistant genes, where this gene–gene interaction (GGI) produced four gene clusters based on four interacting genes of *K. pneumoniae*. MarA, BaeR, and RsmA are the significant resistance-inducing genes as they instigate at least ten neighboring genes (Fig. 2). In gram-negative bacteria, the transcription factor MarA regulates efflux pump production and biofilm formation. Figure 2A shows that MarA (yellow circle) dispatch signals to other AraC transcription activator family members, such as AdaA, Ara, and RhaR, and multiple antibiotic resistance operons, such as MarR and MarC. These transcription regulators are vital in inducing antibiotic resistance in gram-negative and gram-positive bacteria. The CRP protein of the CRP/FNR family is one of the global regulators which takes part in cell division, cell survival, and stress management (Fig. 2B). From the STRING analysis, it's prominent that CRP takes the signal from several DNA-directed rna polymerases (Rpo family) to facilitate transcription, as the report suggests [58]. BaeR gene is a two-component regulatory system that is involved in multidrug resistance and flagellum formation in gram-negative bacteria by inducing signals to other catabolic genes (Fig. 2C). Lastly, the RsmA gene plays a vital role in bacterial ribosomal subunit 30S biosynthesis along with initiating chaperone formation (SurA) and outer lipomembrane synthesis (LptD) (Fig. 2D).

Annotating the virulence genes considering their protein–protein interaction (PPI)

In this study, four genes have been identified as the virulence factors of *K. pneumoniae* strain BR-MHR521, among which the DjlA protein encoding the DnaJ gene has been identified as the most virulent. From the STRING analysis, DjlA-mediated protein interaction has been found with other proteins involved in chaperone activity (Fig. 3), cell survival, biofilm formation, and protein folding. Recent studies corroborated this Djla protein's involvement in virulence in *E. coli* [59].

Evolutionary relationship of DjlA chaperone protein with the common CbpA-inducing macromolecules

According to the phylogenetic analysis, of DjlA chaperone protein (Accession: WP_008807470.1) of *K. pneumoniae* produce a crucial evolutionary relationship with several chaperone heat shock proteins from different strains of *Klebsiella* (Fig. 4A). All these DjlA chaperone from different *Klebsiella* strains can be highly significant in promoting antibiotic resistance, cell survival, and biofilm formation. Chaperone heat shock proteins are found to have Protein folding, and the preservation of protein integrity is helped by chaperones [60]. Thus, they support inherited antimicrobial resistance by having the rare capacity to sustain resistance directly conferring amino acid substitutions in drug targets and mitigating the stress these substitutions impose (AMR) [61]. In case of infection formation like mastitis, DjlA negatively regulates CbpA, one of the most significant Dna-J analogs. Here, CbpA is mainly provoked by three protein molecules when clustered inside the cellular environment, which are DnaK, GrpE, and HscA proteins from the PPI of DjlA [62]. The DjlA-stimulated CbpA protein then starts to function in progressing mastitis rapidly among the subjects [63, 64].

Pharmacokinetic profiles of the target ligands considering their ADMET and QSAR properties

The ADMET analysis revealed major parameters of Lipinski's rules were evaluated based on the drug's molecular weight (≤ 500), H-bond donors (≤ 5), H-bond acceptors (≤ 10), and partition coefficient (log P) (≤ 5). In this study, five ligands were chosen from 200 compound libraries as these compounds did not violate Lipinski's rules [44, 45]. The molecular weight of all five ligands, including the control Galangin, was between 270 and 320. Myricetin has the highest H-bond acceptor [46] and donor [43] values, in addition to its higher blood–brain permeability value (-1.4) among all ligands (Table 1). In a study, Myricetin showed increased bioavailability when co-administered with another drug [65]. Intestinal epithelium absorption (IA) is another ADMET parameter that estimates the amount of orally administered drug absorbed through the gut epithelium [66]. The IA values varied among the ligands, where the control Galangin and ligand Biochanin A showed more than 90% absorption (Table 1). Total Clearance (TC) estimates the dosage rate and drug dosage at a stable state [67]. In this study, the total clearance range of the ligands falls between 0.25 and 0.477, where Kaempherol showed the highest value. All the ligands showed good potential as drug candidates based on their pharmacokinetic profiling [67].

The quantitative structure analysis (QSAR) of all the test ligands was completed using the PASS server to determine their anti-infective, antiviral, and antimicrobial parameters [34, 44]. Three activity parameters of all the test ligands were assessed: the drug candidates' anti-infective, antiviral, and antibacterial properties. All the ligands showed anti-infective and antibacterial characteristics, while there were some discrepancies in the case of antiviral properties. On the PASS server, antiviral activities of the chemical compound are assessed against several viruses such as HIV, Herpes, Influenza. The Pa range of Biochanin A and the control ligand Galangin fell within 0.3 to 0.7 for all the viruses, whereas other ligands outranged those values (Table 2).

Quantum tunneling of CbpA receptor

Previously, quantum tunneling of electrons was evident in enzyme function during viral invasion [36] and a substrate hydrogen atom toward the ferric-hydroxide cofactor, on its active site [68]. After generating quantum tunnel clusters, the two most viable tunnel clusters were identified from the protein's binding active site (Fig. 5B, C). The quantitative approach (Fig. 5A) uses the radius and tunnel length as dependent and independent variables to determine the ligand's length, width, and height [69]. Mean tunnel length, curvature, and bottleneck radius are the prime prerequisites for predicting the super-docking position of the active site with the best binding affinities in a protein [34, 36].

The tunnel cluster-1 sub-tunnels have a bottleneck radius (BR) of 2.3 Å, a curvature of 1.05 Å, and a length of 1.47 Å (Fig. 5B). The length of the manifolds in tunnel cluster 1 is significantly less than in cluster 2. The bottleneck radius (BR) of tunnel cluster 1 is more significant than that of Cluster 2. 52 ILE, 32 MET, 31 GLY, and 33*E are among the amino acid residues present at the tunnel cluster 1 bottleneck point. The tunnel was discovered to be encircled by amino acid residues as the ligand passed through it. Hence, there is a lower likelihood of super docking in these sub-tunnels (Fig. 5B). Conversely, the seven sub-tunnels of cluster 2 have a mean length of 9.56 Å, mean curvature of 1.93 Å and mean bottleneck radius (BR) of 1.02 Å. Tunnel Cluster 2 has a high length with comparatively higher curvature (Fig. 5A). Moreover, along with more amino acid residues engaged, cluster 2 sub-tunnels can be considered better active sites for testing sample ligands, a scenario evident previously [34, 36]. Past research showed that a selection of active sites inside the hACE2 receptor protein for quantum tunneling was based on a high number of amino acid residues and low binding energy [46]. It also supports the study where constituent amino acid residues and protein structure impact efficient multi-peptide electron transport [36]. In this study, tunnel cluster 2 has been found to have seven amino acid residues (53Val, 53Ile, *2Me, 56A**, 55Arg, 74Leu, 70Ile) at the bottleneck area. So, these sub-tunnels are more suitable for forming H-bond with ligands and binding affinities (Fig. 5B).

Point-specific molecular docking and post-docking analysis of the ligand–protein complexes

The supramolecular docking of the five ligand–protein complexes, including the control Galangin, indicated different binding affinities and a range of RMSD values for each docked complex (Table 4). Based on these scores, this study shows that the control ligand Galangin and the test ligand Biochanin A have the lowest binding affinity compared to other test ligands where Myricetin has the highest affinity, so it is deduced that Myricetin is superior to the rest of the other ligands [47, 70]. In contrast to the docking affinity score of ligand–protein complexes, the MMGBSA α-DG score was quite the opposite (Table 4). In this study, Myricetin showed the lowest MMGBSA α-DG value (− 26.11), whereas Quercetin holds the highest value (− 43.15). Several studies showed that a higher negative value is essential for maintaining stability within the ligand–protein complexes after the molecular dynamic simulation [70, 71].

In addition, Kaempferol showed the highest number of hydrogen bonds among all ligands (Fig. 6B), followed by Myricetin (Fig. 6D), Quercetin (Fig. 6E), and lastly Biochanin A (Fig. 6C), which had the least number of hydrogen bonds. The more H-bonds formed, the better because hydrogen bonds are crucial in stabilizing the protein–ligand complex [71]. This bond formation explains the most stable interactive complex between Kaempferol and 3UCS compared to the other ligand–protein interactions in this study. The lesser atomic distance between ligand and amino acid residues makes the interactions relatively anchored. However, in the case of hydrophobic interactions, Quercetin predominates Kaempferol and other candidate ligands with the closest contiguity with six amino acid residues. The control ligand Galangin contains four hydrophobic bonds with His100, Phe97, Leu94, and Arg93 amino acid residues of CbpA (Table 4). Although hydrophobic interactions also contribute to the stability of the protein–ligand complex [43, 47], hydrogen bonds have a more significant effect, making Kaempferol a more effective ligand in potentially inhibiting the chaperone protein activity.

MDS data annotation (100 ns)

This research uses CbpA for MDS mechanisms to find protein–ligand stability. Here, six parameters (i.e., RMSD, Rg, intramolecular H-bonds, Ligand H-bonds, SASA, and RMSF) were governed to analyze the binding mechanism, structural behavior, and the flexibility of compound up to 100 ns simulation period.

RMSD analysis

From the data, Fig. 7A shows the RMSD value for five different ligands (i.e., Kaempherol, Biochanin A, Myricetin, Quercetin, and Galangin). Here, the RMSD calculates the change in the mean displacement of a subset of atoms for a specific frame relative to a reference frame [36]. This factor is vital in supporting the contrasts among different molecular structures and tapers down the widespread list of predictive configurations to a lesser set [46]. However, among the docked complexes, the one with a more excellent RMSD value is less stable than the others. Besides, the lowest RMSD value of docked complexes would exhibit the

highest stability. From the current research's RMSD (nm) profile, the CbpA-Kaempherol complex showed the lowest RMSD value, which denotes the Kaempherol ligand's highest stability profile [34]. In contrast, the CbpA-Quercetin complex manifested the highest RMSD (nm) value, indicating the lowest stability profile (Fig. 7A).

Rg analysis

The radius of gyration (Rg) value indicates protein structure compactness [45]. An increased Rg value indicates a decrease in protein structural compactness, which implies higher flexibility and less stability, and vice versa [72]. In this criterion, the CbpA-Myricetin complex exhibited the highest Rg value, which indicates that the ligand is flexible but less stable. On the contrary, the CbpA-Biochanin A complex pointed lowest Rg value, demonstrating that this ligand is less flexible but more stable than other docked complexes. Biochanin A would be a model ligand of this nature regarding Rg (nm) value (Fig. 7B).

Intermolecular and intramolecular H-bonds

A comprehensive intramolecular hydrogen bond formation and intermolecular hydrogen bond (Ligand H-bonds) formation between the five ligands and DjlA were calculated from the 100 ns trajectory. The relevance of a drug-receptor complex is directly proportional to the number of hydrogen bonds it has formed, as the strength of the binding affinity of the protein and the ligand dramatically depends on the hydrogen bond network [73]. The more the bonds have been formed, the more it is considered ideal [34, 36, 46, 47]. The number of hydrogen bonds formed by Galangin ranged between 62 and 90. In the case of Biochanin A, the number of hydrogen bonds was 60 to 87. For Kaempferol, Myricetin, and Quercetin, the quantity of hydrogen bonds ranged between 61 to 91, 59 to 84, and 59 to 90, respectively (Fig. 7C). These findings stipulate that Quercetin formed the maximum number of hydrogen bonds; as a result, Quercetin has the potential to be used against *Klebsiella pneumoniae*. Intra and intermolecular hydrogen bonds play critical roles in conferring binding specificity and consequently strengthening binding affinities of macromolecule-ligand complexes (i.e., CbpA-ligand complexes in this study) [73, 74].

The ligand hydrogen bond, depicted in Fig. 7D, is an essential parameter in identifying the DjlA–ligands' interaction characteristics in MDS analysis [75]. In our study, the Quercetin–CbpA and Myricetin-CbpA complexes showed the highest number of ligand hydrogen bond interactions among all ligands, including the control Galangin. This result indicates that these two ligand complexes were the most stable ones during the 100 ns of the simulation period. The control complex, Galangin-CbpA formed three ligand hydrogen bonds. On the other hand, Biochanin A and Kaempherol exhibited slightly lower stability than the control as these two ligands formed the least number of hydrogen bonds. These findings indicate that Quercetin–CbpA and Myricetin-CbpA complexes are relatively more stable among all the five complexes studied in this molecular dynamic simulation.

SASA analysis

Table 5 explains the results of SASA for five ligands bound to the CbpA macromolecule. The table also provides the Solvent Accessible Surface Area (SASA) data for various ligands bound to the macromolecule CbpA. The SASA values are reported in terms of Water Probe Radius (WPR), Generalized Born Implicit Solvent Constant (GIC), Total Nonpolar Residue (TNR) area, as well as the number of solvent-accessible atoms (NSA), the number of buried atoms (NBA), and the total area/energy for polar, apolar, and unknown residues [76]. The SASA values indicate the extent to which the ligand is exposed to the solvent and the macromolecule's hydrophobic core [34, 47].

The higher the SASA values, the more exposed the ligand is to the solvent. The lower the SASA values, the more buried the ligand is within the macromolecule's hydrophobic core [70]. The data shows that all the ligands have similar SASA values, indicating that they are all equally accessible to the solvent. The Total Area/Energy column provides information on the ligands' polar, apolar, and unknown residue interactions with the macromolecule. These interactions contribute to the binding affinity and stability of the complex. The data show that the ligands have similar total area/energy values, indicating that they interact similarly with the macromolecule [36]. Overall, the SASA data suggests that all the ligands have similar solvent accessibility and interact similarly with the macromolecule. According to the results, the values of Biochanin A are the greatest, suggesting that it should be accessible for solvents and interact more with solvents. In addition, the SASA values for the five protein complexes (Fig. 8) during MD are relatively stable, indicating no significant changes in the protein structure.

RMSF analysis

The RMSF value can be used to assess how likely a receptor protein is to denature at different points during its temporal trajectory. A higher RMSF value indicates lower stability for the protein–ligand complex during molecular dynamics simulations and vice versa [36]. This is because the ligand interaction can change the protein structure, reflected in higher RMSF values for tightly bonded structures like alpha helices and beta-strands. Conversely, lower RMSF values are associated with looser forms like coils, bends, and turns.

In a recent study, Myricetin was found to have the highest RMSF values compared to other experimental ligands and Quercetin, indicating lower stability due to increased flexibility [34, 47].

On the other hand, the control had the lowest RMSF values, indicating the most stable complex. Additionally, docked complexes containing Galangin, Biochanin A, and Kaempherol were less stable than the control. The fluctuation range of the RMSF values was satisfactory, with the upper and lower ranges representing inferior and robust complex stabilities, respectively. This information is relevant for in silico studies obtained from protein–ligand interactions in viral infections previously [37, 43].

DGI profiling of the target flavonoids

In this study, a group of protein structure regulating genes means CYP2C8, CYP2C18, CYP1A2, CYP3A4, CYP2E1, and CYP2C19 were found to be pharmacodynamically influenced by the Quercetin following its complexing with the CbpA protein (Fig. 9A). Alike, in Myricetin-CbpA complex formation ATK1, PPARG, NR1H3, SIRT1, and PIK3CG genes showed their synergistic effect on Myricetin metabolism (Fig. 9B). Besides, Biochanin A is responsible for interacting the CYP2E1, UGT1A5, UGT1A9, UGT1A7, UGT1A6, UGT1A8, UGT1A4, UGT1A3, UGT1A1, and UGT1A10 genes for the metabolic purpose (Fig. 9C). Surprisingly, Kaempferol formed the most viable and significant DGI, a group protein-activity modulating genes like UGT1A7, UGT1A2. UGT1A8, UGT1A6, UGT1A5, UGT1A3, UGT1A11, UGT1A1, UGT1A10, UGT1A4, UGT2B7, and UGT2B28 were involved (Fig. 9D). On the other hand, the control ligand Galangin impacts on the UGT1A3, UGT1A4, UGT1A7, UGT1A1, UGT1A9, UGT1A6, UGT1A8, UGT1A10, and GSTM1 genes (Fig. 9E). Previously, many experiments were conducted to determine the actual pharmacodynamic potentialities of the natural flavonoids following the molecular docking and dynamic simulation steps, where DGI and DPI (drug-protein interaction) were strongly recommended [30, 34, 36]. It's been reported that flavonoids like Myricetin, Quercetin, and Kaempferol are very effective against viral and bacterial infections in both humans and animals, where the DGI properties were studied repeatedly [77]. Besides, Galangin has been emphasized in formulating target-specific drug development in several recent experiments on mastitis models [77, 78].

Though natural flavonoids have been suggested in formulating drugs for mastitis, different antimicrobial peptides especially bacteriocins are currently emphasized to introduce in preventing the mastitis-causing *K. pneumoniae* and other microbial infections relating to it [79]. Recently, antimicrobial proteins mean that lantibiotics are very effective against contagious zoonotic viral infections [80] including SARS-Cov-2. Surprisingly, many of those antimicrobial proteins were biosynthesized from a wide range of probiotic microorganisms used as nutritional supplements [81], and different food-born fungal strains [82]. It is reported that both plant-derived phytochemicals like flavonoids and biosynthesized antimicrobial proteins can significantly induce the secondary immune response through positive opsonization [83], and this opsonization reinforces the activity of other biological preparations against infections like HAMLET-based control of the cancer cell lines [84]. Besides, natural flavonoids can suppress ROS-mediated cancer formation [85] where the proteins like CbpA, DjlA, and DnaK act as the proton-switch of cellular metabolism and novel targets for drugs.

Conclusion

The current study has revealed the whole genome sequence of the recent-most identified *K. pneumoniae* strain responsible for severe mastitis infection annotating the antibiotic resistance and virulence factors comprehensively. Significantly, DjlA protein was determined as the Dna-J type chaperon protein domain involving abnormal protein-structure mediation enforcing CbpA protein. Based on the molecular string networks of the genes and proteins regulated with the DjlA, a new novel drug-target CbpA has been studied in response to several selective natural flavonoids. Considering all the pharmacokinetic, and pharmacodynamic properties of the flavonoids, the CbpA receptor can be established as an ideal receptor for targeting therapeutics in alleviating mastitis infection. To be more precise for this research, Kaempferol, Myricetin, and Quercetin are the most potential target-specific therapeutic drugs for the DjlA-induced CbpA receptor based on their hydrogen bond profiles, non-covalent interaction status, and all the molecular dynamic simulation (100 ns) parameters. Besides, the synergistic effects of these flavonoid pharmacophores on different groups of gene clusters have been studied rationally so the impacts of those genes in metabolizing the tested pharmacophores in preventing mastitis infection can be screened.

Limitations

Myricetin produced the highest docking score in molecular docking analysis, but compared with its free binding energy, it showed poor results on MMGBSA. Although the repetition of the docking and simulation for Myricetin was repeated several times, they produced the same results. Besides, the mastitis-bovine milk is more prone to contamination than usual, thus immediate conservation following collection was a challenging task from different regions of

the country. The current synopsis comprises only the in vitro and silico aspects of this research.

Acknowledgements The authors are grateful to BAS-USDA Endowment program; Bangladesh Agricultural University, Mymensingh-2202; Department of Livestock Services (DLS), GoB; QC Lab, DLS, Dhaka; and National Institute of Biotechnology, Savar, Dhaka for their unconditional supports to smooth and successful completion of the research.

Author contributions MHR, SAA made the conceptualization, methodology, and formal analysis. MHR, SAA, MFU, MF, IAS, and KSK prepared the original draft. SAA, AJ, AR, FJ, SAS, FHR, TK conducted the in silico data validation, data analysis, and visualization. SAA, MHR, FHR, and TK conducted the wet-lab works including WGS, PCR, PAGE, MALDI-TOF MS. SAA, MHR, FHR, TK accomplished the in silico data curation, and visualization. SAA, RA, N, SR studied the complicated structural modeling and statistical analysis. SAA, RA, N developed the Infection pathway modeling. MHR, SAA, MFU, AJ checked the literature review, and manuscript editing. MFRK, MBR managed the administrative procedures and ethical clearance. MBR, MFRK, managed the funds for wet-lab activities, while SAA funded the in silico parts. MBR was the Supervisor of the project and playing roles as a corresponding author.

Funding The research is fully funded by the Bangladesh Academy of Science (BAS) and the United States Department of Agriculture (USDA) Endowment Program under the Grant ID: BAS-USDA LS-26/2020 (4th phase). The in silico part of this project is fully sponsored by the RPG Interface Lab (Registration No. 05-060-06021), under the Grant ID: Category-E4-GRP-2021/22 (Phase-2).

Data availability All necessary data are properly conserved by the corresponding author, which will be shared upon reasonable request with the journal authority.

Declarations

Competing interest The authors have no conflict of interest at all with the others.

Ethical approval The ethical approval is authorized by AWEC, Bangladesh Agricultural University, Mymesningh regarding the project titled—"Polyvalent Vaccine Development to Prevent Mastitis in Dairy Cow" with the Grant ID: BAS-USDA LS-26/2020 (4th phase).

References

1. Russo TA, Olson R, Fang C-T et al (2018) Identification of biomarkers for differentiation of hypervirulent *Klebsiella pneumoniae* from classical *K. pneumoniae*. J Clin Microbiol 56:e00776-e818. https://doi.org/10.1128/JCM.00776-18
2. Piperaki E-T, Syrogiannopoulos GA, Tzouvelekis LS, Daikos GL (2017) *Klebsiella pneumoniae*: virulence, biofilm and antimicrobial resistance. Pediatr Infect Dis J 36:1002. https://doi.org/10.1097/INF.0000000000001675
3. Paczosa MK, Mecsas J (2016) *Klebsiella pneumoniae*: going on the offense with a strong defense. Microbiol Mol Biol Rev MMBR 80:629–661. https://doi.org/10.1128/MMBR.00078-15
4. Gonzalez-Ferrer S, Peñaloza HF, Budnick JA et al (2021) Finding order in the chaos: outstanding questions in *Klebsiella pneumoniae* pathogenesis. Infect Immun 89:e00693-e720. https://doi.org/10.1128/IAI.00693-20
5. Hu Y, Anes J, Devineau S, Fanning S (2021) *Klebsiella pneumoniae*: prevalence, reservoirs, antimicrobial resistance, pathogenicity, and infection: a hitherto unrecognized zoonotic bacterium. Foodborne Pathog Dis 18:63–84. https://doi.org/10.1089/fpd.2020.2847
6. Mohd Asri NA, Ahmad S, Mohamud R et al (2021) Global prevalence of nosocomial multidrug-resistant *Klebsiella pneumoniae*: a systematic review and meta-analysis. Antibiotics 10:1508. https://doi.org/10.3390/antibiotics10121508
7. David S, Reuter S, Harris SR et al (2019) Epidemic of carbapenem-resistant *Klebsiella pneumoniae* in Europe is driven by nosocomial spread. Nat Microbiol 4:1919. https://doi.org/10.1038/s41564-019-0492-8
8. Rastegar S, Moradi M, Kalantar-Neyestanaki D et al (2019) Virulence factors, capsular serotypes and antimicrobial resistance of hypervirulent *Klebsiella pneumoniae* and classical *Klebsiella pneumoniae* in Southeast Iran. Infect Chemother. https://doi.org/10.3947/ic.2019.0027
9. Holden VI, Breen P, Houle S et al (2016) *Klebsiella pneumoniae* siderophores induce inflammation, bacterial dissemination, and HIF-1α stabilization during pneumonia. MBio 7:e01397. https://doi.org/10.1128/mBio.01397-16
10. Navon-Venezia S, Kondratyeva K, Carattoli A (2017) *Klebsiella pneumoniae*: a major worldwide source and shuttle for antibiotic resistance. FEMS Microbiol Rev 41:252–275. https://doi.org/10.1093/femsre/fux013
11. Dong N, Yang X, Zhang R et al (2018) Tracking microevolution events among ST11 carbapenemase-producing hypervirulent *Klebsiella pneumoniae* outbreak strains. Emerg Microbes Infect 7:1–8. https://doi.org/10.1038/s41426-018-0146-6
12 Tang M, Kong X, Hao J, Liu J (2020) Epidemiological characteristics and formation mechanisms of multidrug-resistant hypervirulent *Klebsiella pneumoniae*. Front Microbiol. https://doi.org/10.3389/fmicb.2020.581543
13 Lee C-R, Lee JH, Park KS et al (2017) Antimicrobial resistance of hypervirulent *Klebsiella pneumoniae*: epidemiology, hypervirulence-associated determinants, and resistance mechanisms. Front Cell Infect Microbiol. https://doi.org/10.3389/fcimb.2017.00483
14. Hua Y, Wang J, Huang M et al (2022) Outer membrane vesicles-transmitted virulence genes mediate the emergence of new antimicrobial-resistant hypervirulent *Klebsiella pneumoniae*. Emerg Microbes Infect 11:1281–1292. https://doi.org/10.1080/22221751.2022.2065935
15. Hou M, Chen N, Dong L et al (2022) Molecular epidemiology, clinical characteristics and risk factors for bloodstream infection of multidrug-resistant *Klebsiella pneumoniae* infections in pediatric patients from Tianjin, China. Infect Drug Resist 15:7015–7023. https://doi.org/10.2147/IDR.S389279
16. Gato E, Vázquez-Ucha JC, Rumbo-Feal S et al (2020) Kpi, a chaperone-usher pili system associated with the worldwide-disseminated high-risk clone *Klebsiella pneumoniae* ST-15. Proc Natl Acad Sci USA 117:17249–17259. https://doi.org/10.1073/pnas.1921393117
17. Moo C-L, Osman MA, Yang S-K et al (2021) Antimicrobial activity and mode of action of 1,8-cineol against carbapenemase-producing *Klebsiella pneumoniae*. Sci Rep 11:20824. https://doi.org/10.1038/s41598-021-00249-y
18. Pranavathiyani G, Prava J, Rajeev AC, Pan A (2020) Novel target exploration from hypothetical proteins of *Klebsiella pneumoniae* MGH 78578 reveals a protein involved in host-pathogen interaction. Front Cell Infect Microbiol. https://doi.org/10.3389/fcimb.2020.00109
19 Wickner S, Camberg JL, Doyle SM, Johnston DM (2017) Molecular chaperones. Reference module in life sciences. Elsevier, Amsterdam

20. Benedetti F, Cocchi F, Latinovic OS et al (2020) Role of mycoplasma chaperone DnaK in cellular transformation. Int J Mol Sci 21:1311. https://doi.org/10.3390/ijms21041311
21 Mayer MP (2021) The Hsp70-chaperone machines in bacteria. Front Mol Biosci. https://doi.org/10.3389/fmolb.2021.694012
22. Moses MA, Zuehlke AD, Neckers L (2018) Molecular chaperone inhibitors. In: Binder RJ, Srivastava PK (eds) Heat Shock proteins in the immune system. Springer, Cham, pp 21–40
23. Chengolova Z, Ivanov Y, Grigorova G (2021) The relationship of bovine milk somatic cell count to neutrophil level in samples of cow's milk assessed by an automatic cell counter. J Dairy Res 88:330–333. https://doi.org/10.1017/S0022029921000534
24. Alhussien MN, Dang AK (2018) Impact of different seasons on the milk somatic and differential cell counts, milk cortisol and neutrophils functionality of three Indian native breeds of cattle. J Therm Biol 78:27–35. https://doi.org/10.1016/j.jtherbio.2018.08.020
25. Al Azad S, Moazzem Hossain K, Rahman SMM et al (2020) In ovo inoculation of duck embryos with different strains of Bacillus cereus to analyse their synergistic post-hatch anti-allergic potentialities. Vet Med Sci 6:992–999. https://doi.org/10.1002/vms3.279
26. Azad SA, Farjana M, Mazumder B et al (2019) Molecular identification of a *Bacillus cereus* strain from Murrah buffalo milk showed in vitro bioremediation properties on selective heavy metals. J Adv Vet Anim Res 7:62–68. https://doi.org/10.5455/javar.2020.g394
27. Lou W, Venkataraman S, Zhong G et al (2018) Antimicrobial polymers as therapeutics for treatment of multidrug-resistant *Klebsiella pneumoniae* lung infection. Acta Biomater 78:78–88. https://doi.org/10.1016/j.actbio.2018.07.038
28. Saleem M, Syed Khaja AS, Hossain A et al (2022) Molecular characterization and antibiogram of acinetobacter baumannii clinical isolates recovered from the patients with ventilator-associated pneumonia. Healthcare 10:2210. https://doi.org/10.3390/healthcare10112210
29. Nonnemann B, Lyhs U, Svennesen L et al (2019) Bovine mastitis bacteria resolved by MALDI-TOF mass spectrometry. J Dairy Sci 102:2515–2524. https://doi.org/10.3168/jds.2018-15424
30. Islam S, Farjana M, Uddin MR et al (2022) Molecular identification, characterization, and antagonistic activity profiling of *Bacillus cereus* LOCK 1002 along with the in-silico analysis of its presumptive bacteriocins. J Adv Vet Anim Res 9:663–675. https://doi.org/10.5455/javar.2022.i635
31. Wick RR, Judd LM, Gorrie CL, Holt KE (2017) Unicycler: Resolving bacterial genome assemblies from short and long sequencing reads. PLOS Comput Biol 13:e1005595. https://doi.org/10.1371/journal.pcbi.1005595
32. Alcock BP, Huynh W, Chalil R et al (2023) CARD 2023: expanded curation, support for machine learning, and resistome prediction at the comprehensive antibiotic resistance database. Nucleic Acids Res 51:D690–D699. https://doi.org/10.1093/nar/gkac920
33. Chen C-Y, Clark CG, Langner S et al (2020) Detection of antimicrobial resistance using proteomics and the comprehensive antibiotic resistance database: a case study. Proteom Clin Appl 14:e1800182. https://doi.org/10.1002/prca.201800182
34. Morshed AKMH, Al Azad S, Mia MdAR et al (2022) Oncoinformatic screening of the gene clusters involved in the HER2-positive breast cancer formation along with the in silico pharmacodynamic profiling of selective long-chain omega-3 fatty acids as the metastatic antagonists. Mol Divers. https://doi.org/10.1007/s11030-022-10573-8
35. Huang JK, Carlin DE, Yu MK et al (2018) Systematic evaluation of molecular networks for discovery of disease genes. Cell Syst 6:484-495.e5. https://doi.org/10.1016/j.cels.2018.03.001
36. Jabin A, Uddin MF, Al Azad S et al (2023) Target-specificity of different amyrin subunits in impeding HCV influx mechanism inside the human cells considering the quantum tunnel profiles and molecular strings of the CD81 receptor: a combined in silico and in vivo study. Silico Pharmacol 11:8. https://doi.org/10.1007/s40203-023-00144-6
37. Sharif MA, Hossen MS, Shaikat MM, et al (2021) Molecular optimization, docking and dynamic simulation study of selective natural aromatic components to block E2-CD81 complex formation in predating protease inhibitor resistant HCV influx. Int J Pharm Res. https://doi.org/10.31838/ijpr/2021.13.02.408
38. Chen L, Zheng D, Liu B et al (2016) VFDB 2016: hierarchical and refined dataset for big data analysis–10 years on. Nucleic Acids Res 44:D694-697. https://doi.org/10.1093/nar/gkv1239
39. Liu B, Zheng D, Zhou S et al (2021) VFDB 2022: a general classification scheme for bacterial virulence factors. Nucleic Acids Res 50:D912–D917. https://doi.org/10.1093/nar/gkab1107
40. Azad S, Ahmed S, Biswas P et al (2022) Quantitative analysis of the factors influencing IDA and TSH downregulation in correlation to the fluctuation of activated vitamin D3 in women. J Adv Biotechnol Exp Ther 5:320. https://doi.org/10.5455/jabet.2022.d118
41. Lemoine F, Correia D, Lefort V et al (2019) NGPhylogeny.fr: new generation phylogenetic services for non-specialists. Nucleic Acids Res 47:W260–W265. https://doi.org/10.1093/nar/gkz303
42. Gialama D, Delivoria DC, Michou M et al (2017) Functional requirements for DjlA- and RraA-mediated enhancement of recombinant membrane protein production in the engineered *Escherichia coli* strains SuptoxD and SuptoxR. J Mol Biol 429:1800–1816. https://doi.org/10.1016/j.jmb.2017.05.003
43. Dey D, Paul PK, Al Azad S et al (2021) Molecular optimization, docking, and dynamic simulation profiling of selective aromatic phytochemical ligands in blocking the SARS-CoV-2 S protein attachment to ACE2 receptor: an in silico approach of targeted drug designing. J Adv Vet Anim Res 8:24–35. https://doi.org/10.5455/javar.2021.h481
44. Arefin A, Ismail Ema T, Islam T et al (2021) Target specificity of selective bioactive compounds in blocking α-dystroglycan receptor to suppress Lassa virus infection: an in silico approach. J Biomed Res 35:459–473. https://doi.org/10.7555/JBR.35.20210111
45. Ferdausi N, Islam S, Rimti FH et al (2022) Point-specific interactions of isovitexin with the neighboring amino acid residues of the hACE2 receptor as a targeted therapeutic agent in suppressing the SARS-CoV-2 influx mechanism. J Adv Vet Anim Res 9:230–240. https://doi.org/10.5455/javar.2022.i588
46. Nipun TS, Ema TI, Mia MdAR et al (2021) Active site-specific quantum tunneling of hACE2 receptor to assess its complexing poses with selective bioactive compounds in co-suppressing SARS-CoV-2 influx and subsequent cardiac injury. J Adv Vet Anim Res 8:540–556. https://doi.org/10.5455/javar.2021.h544
47. Paul PK, Al Azad S, Rahman MH et al (2022) Catabolic profiling of selective enzymes in the saccharification of non-food lignocellulose parts of biomass into functional edible sugars and bioenergy: an in silico bioprospecting. J Adv Vet Anim Res 9:19–32. https://doi.org/10.5455/javar.2022.i565
48. Akter KM, Tushi T, Jahan Mily S et al (2020) RT-PCR mediated identification of SARS-CoV-2 patients from particular regions of Bangladesh and the multi-factorial analysis considering their pre and post infection health conditions. Biotechnol J Int 24:43–56. https://doi.org/10.9734/bji/2020/v24i630121
49. Hossain A, Proma TS, Raju R et al (2022) Employment-related musculoskeletal complications experienced by the physical therapists in Bangladesh: a comprehensive cross-sectional case study. Bull Fac Phys Ther 27:36. https://doi.org/10.1186/s43161-022-00096-6

50. Islam R, Akter KM, Rahman A et al (2021) The serological basis of the correlation between iron deficiency anemia and thyroid disorders in women: a community based study. J Pharm Res Int 33:69–81. https://doi.org/10.9734/jpri/2021/v33i19A31330
51. Mohammad Rashaduzzaman M, Mohammad Kamrujjaman M, Mohammad Ariful Islam MA et al (2019) An experimental analysis of different point specific musculoskeletal pain among selected adolescent-club cricketers in Dhaka City. Eur J Clin Exp Med. https://doi.org/10.15584/ejcem.2019.4.4
52. Akther T, Rony MKK, Anowar A et al (2021) Comparative analysis of the government investments and revenue from different sectors in Bangladesh and its impact on the development of HRM sectors: a 20 years of study. Int J Bus Manag Soc Res. https://doi.org/10.18801/ijbmsr.100120.58
53 Paul PK, Swadhin HR, Tushi T et al (2022) The Pros and cons of selective renewable energy technologies for generating electricity in the perspective of Bangladesh: A survey-based profiling of issues. Eur J Energy Res 2:1–8. https://doi.org/10.24018/ejenergy.2022.2.2.33
54. He M, Li H, Zhang Z et al (2022) Microbiological characteristics and pathogenesis of *Klebsiella pneumoniae* isolated from hainan black goat. Vet Sci 9:471. https://doi.org/10.3390/vetsci9090471
55. Ackers L, Ackers-Johnson G, Welsh J et al (2020) The role of microbiology testing in controlling infection and promoting antimicrobial stewardship. In: Ackers L, Ackers-Johnson G, Welsh J et al (eds) Anti-microbial resistance in global perspective. Springer, Cham, pp 81–102
56. Chakraborty S, Mohsina K, Sarker PK et al (2016) Prevalence, antibiotic susceptibility profiles and ESBL production in *Klebsiella pneumoniae* and *Klebsiella oxytoca* among hospitalized patients. Period Biol. https://doi.org/10.18054/pb.v118i1.3160
57. Tascini C, Sozio E, Viaggi B, Meini S (2016) Reading and understanding an antibiogram. Ital J Med 10:289–300. https://doi.org/10.4081/itjm.2016.794
58 Liu L, Li F, Xu L et al (2020) Cyclic AMP-CRP modulates the cell morphology of *Klebsiella pneumoniae* in high-glucose environment. Front Microbiol. https://doi.org/10.3389/fmicb.2019.02984
59. Sugimoto S, Yamanaka K, Niwa T et al (2021) Hierarchical model for the role of J-domain proteins in distinct cellular functions. J Mol Biol 433:166750. https://doi.org/10.1016/j.jmb.2020.166750
60. Fay A, Philip J, Saha P et al (2021) The DnaK chaperone system buffers the fitness cost of antibiotic resistance mutations in mycobacteria. MBio 12:e00123. https://doi.org/10.1128/mBio.00123-21
61. Min Y, Xu W, Xiao Y et al (2021) Biomineralization improves the stability of a *Streptococcus pneumoniae* protein vaccine at high temperatures. Nanomed 16:1747–1761. https://doi.org/10.2217/nnm-2021-0023
62. Chae C, Sharma S, Hoskins JR, Wickner S (2004) CbpA, a DnaJ homolog, is a DnaK co-chaperone, and its activity is modulated by CbpM*◆. J Biol Chem 279:33147–33153. https://doi.org/10.1074/jbc.M404862200
63. Rezanejad M, Karimi S, Momtaz H (2019) Phenotypic and molecular characterization of antimicrobial resistance in *Trueperella pyogenes* strains isolated from bovine mastitis and metritis. BMC Microbiol 19:305. https://doi.org/10.1186/s12866-019-1630-4
64. Zastempowska E, Lassa H (2012) Genotypic characterization and evaluation of an antibiotic resistance of *Trueperella pyogenes* (*Arcanobacterium pyogenes*) isolated from milk of dairy cows with clinical mastitis. Vet Microbiol 161:153–158. https://doi.org/10.1016/j.vetmic.2012.07.018
65. Dang Y, Lin G, Xie Y et al (2014) Quantitative determination of myricetin in rat plasma by ultra performance liquid chromatography tandem mass spectrometry and its absolute bioavailability. Drug Res 64:516–522. https://doi.org/10.1055/s-0033-1363220
66. Fatima S, Gupta P, Sharma S et al (2020) ADMET profiling of geographically diverse phytochemical using chemoinformatic tools. Future Med Chem 12:69–87. https://doi.org/10.4155/fmc-2019-0206
67. Parikesit AA, Nurdiansyah R (2021) Natural products repurposing of the H5N1-based lead compounds for the most fit inhibitors against 3C-like protease of SARS-CoV-2. J Pharm Pharmacogn Res 9:730–745
68. Khelfaoui H, Harkati D, Saleh BA (2020) Molecular docking, molecular dynamics simulations and reactivity, studies on approved drugs library targeting ACE2 and SARS-CoV-2 binding with ACE2. J Biomol Struct Dyn. https://doi.org/10.1080/07391102.2020.1803967
69. Sepunaru L, Refaely-Abramson S, Lovrinčić R et al (2015) Electronic transport via homopeptides: the role of side chains and secondary structure. J Am Chem Soc 137:9617–9626. https://doi.org/10.1021/jacs.5b03933
70. Ostermann AI, Koch E, Rund KM et al (2020) Targeting esterified oxylipins by LC–MS—effect of sample preparation on oxylipin pattern. Prostaglandins Other Lipid Mediat 146:106384. https://doi.org/10.1016/j.prostaglandins.2019.106384
71. Chen D, Oezguen N, Urvil P et al (2016) Regulation of protein-ligand binding affinity by hydrogen bond pairing. Sci Adv 2:e1501240. https://doi.org/10.1126/sciadv.1501240
72. Li M, Li D, Tang Y et al (2017) CytoCluster: a cytoscape plugin for cluster analysis and visualization of biological networks. Int J Mol Sci 18:1880. https://doi.org/10.3390/ijms18091880
73. Naha A, Banerjee S, Debroy R et al (2022) Network metrics, structural dynamics and density functional theory calculations identified a novel ursodeoxycholic acid derivative against therapeutic target Parkin for Parkinson's disease. Comput Struct Biotechnol J 20:4271–4287. https://doi.org/10.1016/j.csbj.2022.08.017
74. Malik FK, Guo J (2022) Insights into protein–DNA interactions from hydrogen bond energy-based comparative protein–ligand analyses. Proteins 90:1303–1314. https://doi.org/10.1002/prot.26313
75. Semwal DK, Semwal RB, Combrinck S, Viljoen A (2016) Myricetin: A dietary molecule with diverse biological activities. Nutrients 8:90. https://doi.org/10.3390/nu8020090
76. Mishra A, Ranganathan S, Jayaram B, Sattar A (2018) Role of solvent accessibility for aggregation-prone patches in protein folding. Sci Rep 8:12896. https://doi.org/10.1038/s41598-018-31289-6
77. Jiang M, Zhu M, Wang L, Yu S (2019) Anti-tumor effects and associated molecular mechanisms of myricetin. Biomed Pharmacother 120:109506. https://doi.org/10.1016/j.biopha.2019.109506
78. Bhargava P, Mahanta D, Kaul A et al (2021) Experimental evidence for therapeutic potentials of propolis. Nutrients 13:2528. https://doi.org/10.3390/nu13082528
79. Bennett S, Fliss I, Ben Said L et al (2022) Efficacy of bacteriocin-based formula for reducing staphylococci, streptococci, and total bacterial counts on teat skin of dairy cows. J Dairy Sci 105:4498–4507. https://doi.org/10.3168/jds.2021-21381
80 Dey D, Ema T, Biswas P et al (2021) Antiviral effects of bacteriocin against animal-to-human transmittable mutated SARS-COV-2: a systematic review. Front Agric Sci Eng. https://doi.org/10.15302/J-FASE-2021397
81. Al-Mamun M, Hasan M, Azad S et al (2016) Evaluation of potential probiotic characteristics of isolated lactic acid bacteria from goat milk. Br Biotechnol J 14:1–7. https://doi.org/10.9734/BBJ/2016/26397
82. Azad SA, Mamun MAA, Mondal KJ et al (2016) Range of various fungal infections to local and hybrid varieties of non-germinated lentil seed in Bangladesh. J Biosci Agric Res 9:775–781. https://doi.org/10.18801/jbar.090116.93

83 Azad SA, Shahriyar S, Mondal KJ (2016) Opsonin and its mechanism of action in secondary immune response. J Mol Stud Med Res 1:48–56. https://doi.org/10.18801/jmsmr.010216.06
84. Azad SA, Khan I, Salauddin AA, Khan I (2019) HAMLET (human alpha-lactalbumin made lethal to tumor cells)—a hope for the cancer patients. Adv Pharmacol Clin Trials 4(1):000152
85. Biswas P, Dey D, Biswas PK et al (2022) A comprehensive analysis and anti-cancer activities of quercetin in ROS-mediated cancer and cancer stem cells. Int J Mol Sci 23:11746. https://doi.org/10.3390/ijms231911746

IVYSPRING INTERNATIONAL PUBLISHER

Journal of Genomics

2024; 12: 19-25. doi: 10.7150/jgen.90833

Research Paper

Molecular identification and whole genome sequence analyses of methicillin-resistant and mastitis-associated *Staphylococcus aureus* sequence types 6 and 2454 isolated from dairy cows

Mohammad H. Rahman[1,#], Mohamed E. El Zowalaty[2,#,✉], Linda Falgenhauer[3], Mohammad F. R. Khan[1], Jahangir Alam[4], Najmun N. Popy[1], Hossam Ashour[5], Md. Bahanur Rahman[1,✉]

1. Dept. of Microbiology and Hygiene, Bangladesh Agricultural University, Mymensingh-2202, Bangladesh.
2. Veterinary Medicine and Food Security Research Group, Medical Laboratory Sciences Program, Faculty of Health Sciences, Abu Dhabi Women's Campus, Higher Colleges of Technology, Abu Dhabi, UAE.
3. Institute of Hygiene and Environmental Medicine, Justus Liebig University Giessen, Biomedical research center Seltersberg, Schubertstrasse 81, 35392 Giessen, Germany.
4. National Institute of Biotechnology, Savar, Dhaka, Bangladesh.
5. Department of Integrative Biology, College of Arts and Sciences, University of South Florida, St. Petersburg, Florida, USA.

Mohammad H. Rahman and Mohamed E. El Zowalaty are equal first authors and were arranged by order of increasing seniority.

✉ Corresponding author: MEZ; elzow005@gmail.com and bahanurr@bau.edu.bd.

Received: 2023.10.07; Accepted: 2023.12.19; Published: 2024.01.01

Abstract

The emergence of antimicrobial-resistant and mastitis-associated *Staphylococcus aureus* is of great concern due to the huge economic losses worldwide. Here, we report draft genome sequences of two *Staphylococcus aureus* strains which were isolated from raw milk samples obtained from mastitis-infected cows in Bangladesh. The strains were isolated and identified using conventional microbiological and molecular PCR methods. Antibiotic susceptibility testing was performed. Genomic DNA of the two strains was extracted and the strains were sequenced using Illumina NextSeq 550 platform. The assembled contigs were analyzed for virulence determinants, antimicrobial resistance genes, extra-chromosomal plasmids, and multi-locus sequence type (MLST). The genomes of the two strains were compared to other publicly available genome sequences of *Staphylococcus aureus* strains, and raw read sequences were downloaded and all sequence files were analyzed identically to generate core genome phylogenetic trees. The genome of BR-MHR281strain did not harbour any antibiotic resistance determinants, however BR-MHR220 strain harbored *mecA* and *blaZ* genes. Analysis of BR-MHR220 strain revealed that it was assigned to sequence type (ST-6), clonal complex (CC) 5 and *spa* type t304, while BR-MHR281 strain belonged to ST-2454, CC8, and harbored the *spa* type t7867. The findings of the present study and the genome sequences of BR-MHR220 and BR-MHR281 strains will provide data on the detection and genomic analysis and characterization s of mastitis-associated *Staphylococcus aureus* in Bangladesh. In addition, the findings of the present study will serve as reference genomes for future molecular epidemiological studies and will provide significant data which help understand the prevalence, pathogenesis and antimicrobial resistance of mastitis-associated *Staphylococcus aureus*.

Introduction

Bovine mastitis is a multi-factorial, multi-etiological, highly contagious common livestock production-related disease. Bovine mastitis causes huge economic losses and leads to great implications in dairy industry worldwide due to the reduced milk quality and quantity in dairy herds [1]. Mastitis is

very complex and multi-etiological disease caused by more than 140 species of bacteria [2].

Staphylococcus aureus (*S. aureus*) is one of the major foodborne pathogens associated with various human infections and animal diseases including important livestock such as cattle, cows, sheep and goats [3]. *S. aureus* is the most common etiological agent associated with bovine mastitis worldwide and results in a range of manifestations, including a large proportion of subclinical and chronic infections [4,5]. Among livestock, cows are a common reservoir of *S. aureus,* and dairy cattle frequently experience clinical and subclinical mastitis due to *S. aureus* intra-mammary infections [6].

S. aureus possesses an arsenal of virulence and antimicrobial resistance determinants which are subject to horizontal genetic transfer and recombination [7]. Genome sequencing has provided insight into the genotypic features of various *S. aureus* clones worldwide, delivering more options for developing therapeutics and molecular diagnostic tools to detect resistant and difficult-to-treat strains.

Genome sequencing and characterization of *S. aureus* isolated from bovine milk is an important tool in the epidemiological studies of bovine mastitis provide clinically relevant results and contribute to the understanding of the pathogen's dissemination and contagious properties [4,8].

The detection of antimicrobial resistant *S. aureus* strains isolated from bovine mastitis, its zoonotic potential, and the possibility of transmission to humans via the consumption of raw unpasteurized dairy and livestock products are increasing public health concerns [9,10]. Irrational use of antibiotics in bovine mastitis treatment may results in the development of resistant strains and residual antibiotics in milk also pose serious public health concerns [9,11]. The factors, etiologies, treatment, and molecular characterization of common bovine mastitis-causing pathogens were recently reported [12], yet no studies on the application of whole genome sequencing in mastitis-causing pathogens were reported from Bangladesh. Here we report the draft genome sequences of two *S. aureus* strains isolated from raw milk samples obtained from mastitis lactating cows in Bangladesh.

Materials and Methods

Ethics statement

The study protocol entitled "Development of polyvalent mastitis vaccine and probiotics for prevention of mastitis in cows" under the project entitled "Polyvalent Vaccine Development for Mastitis in Dairy Cow" reference number AWEEC/BAU/2020(44) was approved by the Animal Welfare and Experimentation Ethics Committee, Bangladesh Agricultural University, Mymensingh-2202, Bangladesh.

Sample collection

Milk samples were obtained from 36-month and 46-month-old female lactating Holstein Friesian (*Bos taurus taurus*) cows as previously reported [13]. Cow udders were washed with clean water and dried, then the udder teats were rubbed with 70% ethanol. The first two strings were discarded, and California mastitis test was performed to determine the milk somatic cell counts in milk samples as previously reported [13]. Milk samples (10 mL) were collected in sterile tubes and samples were transported to the laboratory maintaining a cold chain for further analysis. Somatic cell counting was performed using Lactoscan Combo's SCC (Milkotronic Ltd, Bulgaria) according to the manufacturer's protocol.

Bacterial isolation

Milk samples (500 µL) were inoculated in 10 mL nutrient broth and incubated at 37°C for 18 hours and subsequently streaked on Mannitol salt agar media (HiMedia). The inoculated plates were incubated at 37 °C for 24 hours and sub-cultured to isolate presumptively identified *S. aureus* pure colonies as previously reported [13].

DNA extraction and bacterial identification using PCR

Presumptive *S. aureus* pure single colonies were confirmed using *S. aureus* primer-specific PCR. Genomic DNA was extracted using genomic DNA Purification Kit (Promega, WI, USA) and isolates were confirmed using PCR using species-specific primers (GCG ATT GAT GGT GAT ACG GTT and AGC CAA GCC TTG ACG AAC TAA AGC) targeting the *nuc* gene as previously reported [14].

Antimicrobial Sensitivity testing

Antimicrobial susceptibility profiles against ciprofloxacin (5µg), Cefoxitin (30µg), chloramphenicol (10µg), doxycycline (30µg), fosfomycin (50µg), gentamicin (10µg), levofloxacin (5µg), sulfamethoxazole - trimethoprim (1.25/23.75µg), and tetracycline (30µg) were determined using the Kirby-Bauer disk diffusion method (Oxoid Ltd., UK), as previously reported. The results were interpreted according to Clinical and Laboratory Standard Institute guidelines [15].

Whole-genome sequencing analysis

S. aureus PCR-confirmed isolates were subjected to Invent Technology Ltd. (Banani, Dhaka, Bangladesh) for whole-genome sequencing as recently

reported [13]. Sequencing libraries were prepared using a Nextera XT library preparation kit (Illumina Inc., CA, USA) and sequencing was performed on the Illumina NextSeq 550 platform (Illumina Inc., CA, USA) using the high-output reagent kit with 150 nt maximal read length.

Bioinformatic analyses

Gene predictions and annotations were performed using the National Center for Biotechnology Information (NCBI) Prokaryotic Genome Annotation Pipeline (PGAP) [16]. Raw paired-end reads were quality checked and assembled to contigs using the ASA^{3}P pipeline [17]. The detection of antibiotic resistance genes was performed using Resfinder 4.0 [18]. SCCmec type determination was performed using the SCCmecFinder tool, (https://cge.food.dtu.dk/services/SCCmecFinder/). Multilocus sequence type determination was performed using PubMLST [19]. *spa* type determination was performed using spaTyper 1.0 [20]. Virulence gene determination was performed using VFanalyzer [21]. The presence of Cap5A-P proteins from *S. aureus* USA300_FPR3757 [22] was determined using tblastN. Core-genome-based analysis was performed using ParSNP of the Harvest Suite package [23]. The resulting trees were annotated using ITol v 6.6 [24].

Results and Discussion

In the present study, a total of 423 randomly selected lactating cows were tested for the detection of *S. aureus* in their milk samples and it was found that 44.68% (189/423) of the cow were mastitis positive, of which 17.49% (74/423) were clinical and 27.19% (115/423) sub-clinical mastitis. Isolation of *S. aureus* was performed using mannitol salt agar which were subsequently confirmed using *nun*-gene specific PCR. It was found that 54.49% (103 out of 189 mastitis affected cows) were infected with *Staphylococcus aureus*.

Genome sequences of two *S. aureus* BR-MHR220 and BR-MHR281strains were generated and raw paired-end reads (average read count 18,863,133; average coverage ×1024, average read length 135 nt) were quality checked and assembled to contigs using the ASA^{3}P pipeline [17]. Assembly was performed using SPAdes v3.13.0 [25] integrated in ASA^{3}P. Contigs smaller than 200 bp were discarded. Contigs were uploaded to NCBI and annotated using the NCBI Prokaryotic Genome Annotation Pipeline v6.0 [16].

For BR-MHR220 genome, a total number of 54 contigs and 2,815,914 bp, with a G+C content of 32.75%, and a N_{50} value of 321,760 bp was achieved. For BR-MHR281 genome, a total number of 28 contigs and 2,728,146 bp, with a G+C content of 32.73%, and a N_{50} value of 470,470 bp was achieved.

Gene predictions and annotations were performed using the National Center for Biotechnology Information (NCBI) Prokaryotic Genome Annotation Pipeline (PGAP), which identified 2,788 coding DNA sequences (CDS), 54 tRNAs, 4 ncRNA and 4 rRNA genes for BR-MHR220, and 2,677 coding DNA sequences, 56 tRNAs, 4 ncRNA and 4 rRNA genes for BR-MHR281.

Phenotypic antimicrobial profiling revealed that both BR-MHR220 and BR-MHR281 strains were resistant to cefoxitin, methicillin, and oxacillin. Additionally, BR-MHR220 strain was resistant to linezolid and penicillin G, while BR-MHR281 strain was resistant to gentamicin and levofloxacin. Both BR-MHR220 and BR-MHR281 strains were sensitive to chloramphenicol, ciprofloxacin, doxycycline, and sulfamethoxazole-trimethoprim. Additionally, BR-MHR220 strain was sensitive to gentamicin and levofloxacin, while BR-MHR281 was strain sensitive to linezolid, penicillin G, and tetracycline.

Genome analyses of the two BR-MHR220 and BR-MHR281 strains were performed and no antibiotic resistance genes were detected in strain BR-MHR281, however strain BR-MHR220 harbored the *mecA* and *blaZ* genes. The *mecA* gene is presumably located on a SCCmec type IVa(2B) element. The reported genotype does not fit to the phenotypic resistance detected. The discrepancy between genotypic and phenotypic resistance may be explained by possible mutations of porin genes or overexpression of efflux pumps.

Only few *S. aureus* STs were previously reported to be positive for *blaZ* or *mecA and s*ome human-adapted lineages, such as ST5 (CC5), ST8 (CC8), and their variants were previously isolated from cows and were positive for *blaZ* and [26-28]. *In the present study, we reported the detection of ST6 (CC5) isolate positive for both blaZ* and *mecA.*

Determination of virulence gene was performed using VFanalyzer [20]. In addition, the presence of Cap5A-P proteins from *S. aureus* USA300_FPR3757 [21] in both BR-MHR220 andBR-MHR281 genomes was determined using tblastN. The overview of detected virulence genes is depicted in Supplementary Table 1. Homologues of 60 virulence genes were detected in both isolates, while specific 19 and 13 virulence genes were only detected in BR-MHR220 and BR-MHR281, respectively. The virulence genes detected only in BR-MHR220 were the cell wall associated fibronectin binding protein *ebh*, the collagen adhesion *cna*, the intracellular adhesin *icaD*, two Ser-Asp rich fibrinogen-binding proteins (*sdrD, sdrE*), six serine proteases (*splA, splB, splC, splD, splE, splF*), Staphylokinase (*sak*), SCIN (*scn*),

Enterotoxin A (*sea*), four Exotoxins (set7, set15, set16, set25) and Leukotoxin D (*lukD*). BR-MHR281 harbored seven enterotoxins (*seg, yent2, selk, selm, seln, selo, selq*). All were different to the one found in BR-MHR220. Five exotoxins were detected only in BR-MHR281 (*set17, set21, set26, set30, set39*). The toxic shock syndrome toxin (*tsst*) was detected only in BR-MHR281.

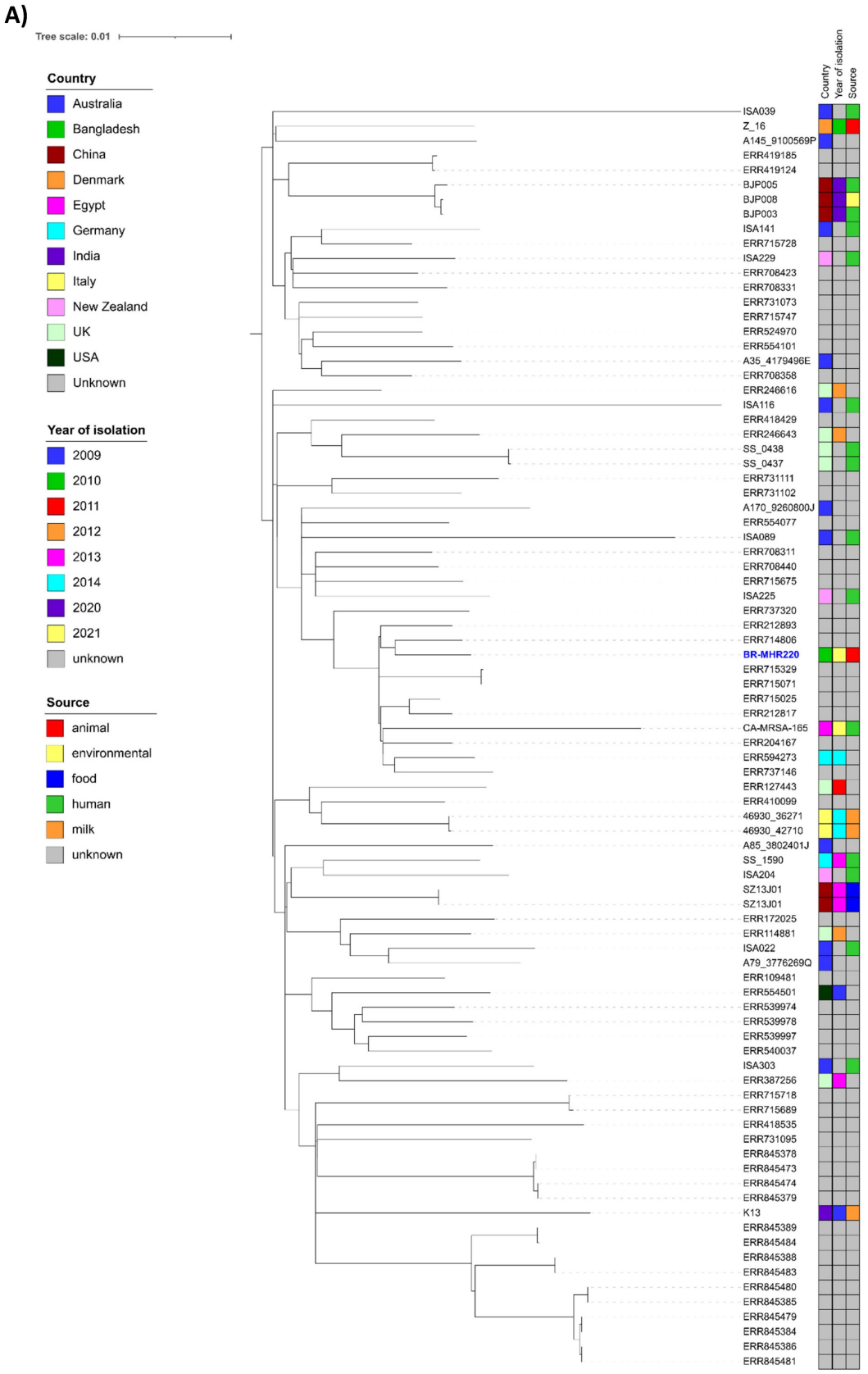

B)

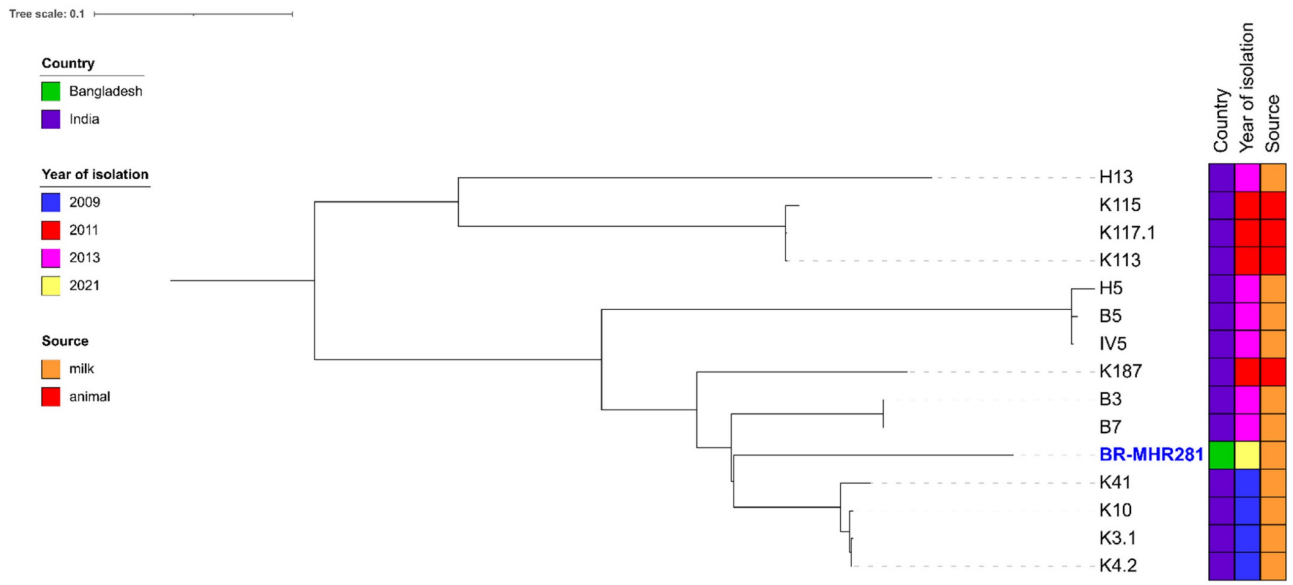

Figure 1: Phylogenetic trees of *S. aureus* strain (A) BR-MHR220 and (B) BR-MHR281. For the core genome-based comparison, ST 6 or ST 2454 sequence information present in PubMLST was used. Trees were annotated using ITOL v. 6.6 and modified using Inkscape.

Multilocus sequence type determination was performed using PubMLST [18]. *spa* type determination was performed using spaTyper 1.0 [19]. BR-MHR220 was assigned to sequence type (ST-6), clonal complex (CC) 5 and *spa* type t304, while BR-MHR281 belonged to ST-2454 and CC8 and harbored the *spa* type t7867.

Several bovine-adapted *S. aureus* lineages including CC97, CC133, and CC151 and human-adapted lineages including CC1, CC5, CC8, CC30, and CC45 were previously reported [29]. In the present study, two strains belonging to CC5 and CC8 *S. aureus* lineages were isolated from bovine mastitis samples. Similarly, the genome sequences of three human-adapted isolates (two from CC97 and one from CC8), isolated from bovine mastitis samples were previously reported [30]. Altogether, this provide significant insights on the role of genomic characteristics in early *S. aureus* host spillover events followed by adaption to a new host. The zooanthroponotic transfer and the spillover transmission of CC5 and CC8 from humans to bovine in the present study are possible events and require further investigation and comparative genomic analysis.

For comparison of BR-MHR220 and BR-MHR281 with global isolates, ST6 (n=85, Supplementary Table 2) and ST2454 (n= 14, Supplementary Table 3) isolate contigs were downloaded from the PubMLST database (as of 23rd January 2023). Core-genome-based analysis was performed using ParSNP of the Harvest Suite package [22]. The resulting trees were annotated using ITol v 6.6 [23]. As depicted in Figure 1A, the closest relative to BR-MHR220 was ERR714806, an isolate collected in the frame of a study on MRSA in England (source unknown) [31]. The closest relative to BR-MHR281 (Figure 1B) was K4.2, isolated from cow milk in India in 2009. The current findings describe the use of whole genome sequencing methods in the detection of bovine mastitis-associated *S. aureus* isolates in dairy cows in Bangladesh, corroborate the worldwide distribution of *S. aureus* CC8 and CC5 isolates in different host species. At present however, WGS still remains unaffordable and inaccessible tool in resource-limited settings. The genome sequences of *S. aureus* strains in the present study will contribute in advanced understanding of the virulence, host adaptation, zoonotic and zooanthroponotic potential of *S. aureus*.

Data availability

This whole-genome sequencing project has been deposited at DDBJ/ENA/GenBank under the BioProject number PRJNA716986 (BioSample accession numbers SAMN26025965 and SAMN26025969 and GenBank accession numbers JALBGM000000000 and JALBGI000000000. The versions described in this paper are the first version. The sequences have been submitted to the Sequence Read Archive (SRA) under the accession numbers SRR18182112 and SRR1818 2108. All isolates used in this study were submitted to Public Databases for molecular typing and microbial genome diversity for curation (https://pubmlst.org/organisms/staphylococcus-aureus) and are publicly

available under PubMLST ID numbers 38059 and 38060.

Supplementary Material

Supplementary tables.
https://www.jgenomics.com/v12p0019s1.pdf

Acknowledgements

The whole-genome sequencing work was supported in part by the Bangladesh Academy of Sciences and the United States Department of Agriculture (Project ID: BAS-USDA LS-26/2020), the Bangladesh Agricultural University Research System (BAURES), and the Hessian Ministry of Higher Education, Research and Arts within the project HuKKH (Hessisches Universitaeres Kompetenzzentrum Krankenhaus Hygiene), Germany. Authors thank the NCBI GenBank submission staff for help with the genome upload, decontamination and deposition process.

Funding

This project was supported in part by the Bangladesh Academy of Sciences and the United States Department of Agriculture (Project ID: BAS-USDA LS-26/2020), the Bangladesh Agricultural University Research System (BAURES), the Hessian Ministry of Higher Education, Research and Arts within the project HuKKH (Hessisches Universitaeres Kompetenzzentrum Krankenhaus Hygiene), Germany and by Monash University Award (I-M010-IRA-000002).

Declaration

No other individual has any role in the study design, analysis of data, writing of the manuscript or decision to publish. The views, opinions, and/or findings expressed are those of the authors and should not be interpreted as representing the official views or policies of the U.S. Department of Agriculture or the U.S. Government.

Author contributions

M.H.R.: Conceptualization, Methodology, Investigation, Formal analysis. MEZ: Conceptualization, Methodology, Data curation, Formal analysis, Investigation, Visualization, Validation, Writing – original draft, Writing – review & editing, Project administration, Supervision; LF: Formal analysis, Methodology, Visualization, Data curation, Software, Validation; Writing – original draft, Writing – review & editing; M.F.R.K.: Methodology, Investigation; J.A.: Methodology, Investigation; N.N.P.: Methodology, Investigation. M.B.R.: Conceptualization, Validation, Funding acquisition, Supervision, Project administration.

M.H.R., J.A., M.E.Z., and M.B.R. designed the experiment. M.H.R., M.F.R.K., and N.N.P. performed sample collection, bacterial culture and preliminary identification of the samples. L.F. analyzed the genomes. L.F. and M.E.Z. analyzed the data. M.E.Z. wrote the initial draft. L.F. and M.E.Z. wrote the manuscript. M.E.Z. critically revised the manuscript. M.B.R. and M.E.Z. supervised the project.

Competing Interests

The authors have declared that no competing interest exists.

References

1. Halasa, T., Huijps, K., Østerås, O. & Hogeveen, H. Economic effects of bovine mastitis and mastitis management: A review. Vet. Q. 29, 18–31 (2007).
2. Pascu C, Herman V, Iancu I and Costina L. 2022 Etiology of Mastitis and Antimicrobial Resistance in Dairy Cattle Farms in the Western Part of Romania. Antibiotics 11: 57
3. Fetsch A, Johler S. Staphylococcus aureus as a foodborne pathogen. Curr Clin Microbiol. 2018; 5(2):88–96.
4. Cremonesi P, Pozzi F, Raschetti M, Bignoli G, Capra E, Graber HU, Vezzoli F, Piccinini R, Bertasi B, Biffani S, Castiglioni B, Luini M. Genomic characteristics of Staphylococcus aureus strains associated with high within-herd prevalence of intramammary infections in dairy cows. J Dairy Sci. 2015;98(10):6828-38. doi: 10.3168/jds.2014-9074.
5. Annamanedi, M., Sheela, P., Sundareshan, S. et al. Molecular fingerprinting of bovine mastitis-associated Staphylococcus aureus isolates from India. Sci Rep 11, 15228 (2021). doi: 10.1038/s41598-021-94760-x
6. Watts JL. Etiological agents of bovine mastitis. Vet Microbiol. 1988;16:41–66. doi: 10.1016/0378-1135(88)90126-5.
7. Chan CX, Beiko RG, Ragan MA. 2011. Lateral transfer of genes and gene fragments in Staphylococcus extends beyond mobile elements. J. Bacteriol. 193:3964–3977
8. Castelani L, et al. Molecular typing of mastitis causing Staphylococcus aureus isolated from heifers and cows. Int J Mol Sci. 2013;14:4326–4333
9. Neelam, Jain VK, Singh M, Joshi VG, Chhabra R, Singh K, et al. (2022) Virulence and antimicrobial resistance gene profiles of Staphylococcus aureus associated with clinical mastitis in cattle. PLoS ONE 17(5): e0264762. doi: 0.1371/journal.pone.0264762.
10. Maity S, Ambatipudi K. Mammary microbial dysbiosis leads to the zoonosis of bovine mastitis: a One-Health perspective, FEMS Microbiology Ecology, Volume 97, Issue 1, 2021, fiaa241, doi: 10.1093/femsec/fiaa241
11. de-Jong A, Garch FE, Simjee S, Moyaert H, Rose M, Youala M, et al. Monitoring of antimicrobial susceptibility of udder pathogens recovered from cases of clinical mastitis in dairy cows across Europe: Vet Path results. Vet Microbiol. 2018; 213:73–81. pmid:29292007
12. Hoque MN, Istiaq A, Clement RA, Sultana M, Crandall KA, Siddiki AZ and Hossain MA. 2019. Metagenomic Deep Sequencing Reveals Association of Microbiome Signature with Functional Biases in Bovine Mastitis. Scientific Reports 9:13536.
13. Rahman MH, El Zowalaty ME, Falgenhauer L, Khan MFR, Alam J, Popy NN, Rahman MB. Draft Genome Sequences of Two Clinical Mastitis-Associated Escherichia coli Strains, of Sequence Type 101 and Novel Sequence Type 13054, Isolated from Dairy Cows in Bangladesh. Microbiol Resour Announc. 2023;12(8):e0016623. doi: 10.1128/mra.00166-23.
14. Ewida RM, Al-Hosary AAT (2020) Prevalence of enterotoxins and other virulence genes of Staphylococcus aureus caused subclinical mastitis in dairy cows. Veterinary World, 13(6): 1193-1198.
15. CLSI (2020) CLSI M100-ED29: 2021 Performance Standards for Antimicrobial Susceptibility Testing, 30th Edition. Vol. 40, PA, USA.
16. Tatusova T, DiCuccio M, Badretdin A, Chetvernin V, Nawrocki EP, Zaslavsky L, Lomsadze A, Kim D, Borodovsky M, Ostell J. 2016. NCBI prokaryotic genome annotation pipeline. Nucleic Acids Res 44:6614–6624. doi: 10.1093/nar/gkw569
17. Schwengers O, Hoek A, Fritzenwanker M, Falgenhauer L, Hain T, Chakraborty T, Goesmann A. ASA3P: An automatic and scalable pipeline for the assembly, annotation and higher-level analysis of closely related bacterial isolates. PLoS Comput Biol. 2020;16(3):e1007134. doi: 10.1371/journal.pcbi.1007134
18. Bortolaia V, Kaas RS, Ruppe E, Roberts MC, Schwarz S, Cattoir V, Philippon A, Allesoe RL, Rebelo AR, Florensa AF, Fagelhauer L, Chakraborty T, Neumann B, Werner G, Bender JK, Stingl K, Nguyen M, Coppens J, Xavier BB, Malhotra-Kumar S, Westh H, Pinholt M, Anjum MF, Duggett NA, Kempf I, Nykäsenoja S, Olkkola S, Wieczorek K, Amaro A, Clemente L, Mossong J, Losch S, Ragimbeau C, Lund O, Aarestrup FM. ResFinder 4.0 for predictions

of phenotypes from genotypes. J Antimicrob Chemother. 2020;75(12):3491-3500. doi: 10.1093/jac/dkaa345.
19. Enright MC, Day NP, Davies CE, Peacock SJ, Spratt BG. Multilocus sequence typing for characterization of methicillin-resistant and methicillin-susceptible clones of Staphylococcus aureus. J Clin Microbiol. 2000;38(3):1008-15. doi: 10.1128/JCM.38.3.1008-1015.2000.
20. Bartels MD, Petersen A, Worning P, Nielsen JB, Larner-Svensson H, Johansen HK, Andersen LP, Jarløv JO, Boye K, Larsen AR, Westh H. Comparing whole-genome sequencing with Sanger sequencing for spa typing of methicillin-resistant Staphylococcus aureus. J Clin Microbiol. 2014;52(12):4305-8. doi: 10.1128/JCM.01979-14.
21. Liu B, Zheng D, Jin Q, Chen L, Yang J. VFDB 2019: a comparative pathogenomic platform with an interactive web interface. Nucleic Acids Res. 2019;47(D1):D687-D692. doi: 10.1093/nar/gky1080.
22. Diep BA, Gill SR, Chang RF, Phan TH, Chen JH, Davidson MG, Lin F, Lin J, Carleton HA, Mongodin EF, Sensabaugh GF, Perdreau-Remington F. Complete genome sequence of USA300, an epidemic clone of community-acquired meticillin-resistant Staphylococcus aureus. Lancet. 2006;367(9512):731-9. doi: 10.1016/S0140-6736(06)68231-7.
23. Treangen TJ, Ondov BD, Koren S, Phillippy AM. The Harvest suite for rapid core-genome alignment and visualization of thousands of intraspecific microbial genomes. Genome Biol. 2014;15(11):524. doi: 10.1186/s13059-014-0524-x.
24. Letunic I, Bork P. Interactive Tree Of Life (iTOL) v5: an online tool for phylogenetic tree display and annotation. Nucleic Acids Res. 2021 ;49(W1):W293-W296. doi: 10.1093/nar/gkab301.
25. Bankevich A, Nurk S, Antipov D, Gurevich AA, Dvorkin M, Kulikov AS, Lesin VM, Nikolenko SI, Pham S, Prjibelski AD, Pyshkin AV, Sirotkin AV, Vyahhi N, Tesler G, Alekseyev MA, Pevzner PA. SPAdes: a new genome assembly algorithm and its applications to single-cell sequencing. J Comput Biol. 2012;19(5):455-77. doi: 10.1089/cmb.2012.0021.
26. Klibi A, Jouini A, Gómez P, Slimene K, Ceballos S, et al. Molecular characterization and clonal diversity of methicillin-resistant and -susceptible Staphylococcus aureus isolates of milk of cows with clinical mastitis in Tunisia. Microb Drug Resist. 2018;24:1210–1216. doi: 10.1089/mdr.2017.0278.
27. Schmidt T, Kock MM, Ehlers MM. Molecular characterization of Staphylococcus aureus isolated from bovine mastitis and close human contacts in South African dairy herds: genetic diversity and inter-species host transmission. Front Microbiol. 2017;8:511. doi: 10.3389/fmicb.2017.00511.
28. Käppeli N, Morach M, Corti S, Eicher C, Stephan R, et al. Staphylococcus aureus related to bovine mastitis in Switzerland: Clonal diversity, virulence gene profiles, and antimicrobial resistance of isolates collected throughout 2017. J Dairy Sci. 2019;102:3274–3281. doi: 10.3168/jds.2018-15317
29. Park S, Ronholm J. Staphylococcus aureus in agriculture: lessons in evolution from a multispecies pathogen. Clin Microbiol Rev. 2021;34:e00182-20. doi: 10.1128/CMR.00182-20
30. Park S, Jung D, O'Brien B, Ruffini J, Dussault F, Dube-Duquette A, Demontier É, Lucier JF, Malouin F, Dufour S, Ronholm J. Comparative genomic analysis of Staphylococcus aureus isolates associated with either bovine intramammary infections or human infections demonstrates the importance of restriction-modification systems in host adaptation. Microb Genom. 2022 Feb;8(2):000779. doi: 10.1099/mgen.0.000779.
31. Toleman MS, Reuter S, Coll F, Harrison EM, Blane B, Brown NM, Török ME, Parkhill J, Peacock SJ. Systematic Surveillance Detects Multiple Silent Introductions and Household Transmission of Methicillin-Resistant Staphylococcus aureus USA300 in the East of England. J Infect Dis. 2016 Aug 1;214(3):447-53. doi: 10.1093/infdis/jiw166.

Journal of Global Antimicrobial Resistance 38 (2024) 111–115

Contents lists available at ScienceDirect

Journal of Global Antimicrobial Resistance

journal homepage: www.elsevier.com/locate/jgar

Genome Note

Draft genome sequences of clinical mastitis-associated *Enterococcus faecalis* and *Enterococcus faecium* carrying multiple antimicrobial resistance genes isolated from dairy cows

Mohammad H. Rahman[a,#], Mohamed E. El Zowalaty[b,#,*], Linda Falgenhauer[c], Mohammad Ferdousur Rahman Khan[a], Jahangir Alam[d], Najmun Nahar Popy[a], Md. Bahanur Rahman[a]

[a] Department of Microbiology and Hygiene, Bangladesh Agricultural University, Mymensingh 2202, Bangladesh
[b] Department of Microbiology and Immunology, Faculty of Pharmacy, Ahram Canadian University, Giza, Egypt
[c] Institute of Hygiene and Environmental Medicine, Justus Liebig University Giessen, Biomedical Research Center Seltersberg, Schubertstrasse 81, 35392 Giessen, Germany
[d] National Institute of Biotechnology, Savar, Dhaka, Bangladesh

ARTICLE INFO

Article history:
Received 12 December 2023
Revised 19 March 2024
Accepted 15 May 2024
Available online 23 May 2024

Editor: Stefania Stefani

Keywords:
Enterococcus faecalis
Enterococcus faecium
Genome sequencing
Mastitis
Antimicrobial resistance

ABSTRACT

Objectives: The emergence of antimicrobial-resistant and mastitis-associated *Enterococcus faecalis* and *Enterococcus faecium* is of great concern due to the huge economic losses associated with enterococcal infections. Here we report the draft genome sequences of *E. faecalis* and *E. faecium* strains that were isolated from raw milk samples obtained from mastitis-infected cows in Bangladesh.

Methods: The two strains were isolated, identified, and genomic DNA was sequenced using the Illumina NextSeq 550 platform. The assembled contigs were analysed for virulence, antimicrobial resistance genes, and multilocus sequence type. The genomes were compared to previously reported *E. faecalis* and *E. faecium* genomes to generate core genome phylogenetic trees.

Results: *E. faecalis* strain BR-MHR218Efa and *E. faecium* strain BR-MHR268Efe belonged to multilocus sequence types ST-190 and ST-22, respectively, both of which appear to represent relatively rare sequence types. BR-MHR268Efe harboured only one antibiotic resistance gene encoding resistance towards macrolides (*lsa*(*A*)), while BR-MHR218Efa harboured ten different antibiotic resistance genes encoding resistance to aminoglycosides (*ant*[6]-Ia, *aph*(3′)-III), sulphonamides (*aac*(6′)-II), lincosamides (*lnu*(*B*)), macrolides (*erm*(*B*)), MLSB antibiotics (*msr*(*C*)), tetracyclines (*tet*(*M*), *tet*(*L*)), trimethoprim (*dfrG*), and pleuromutilin-lincosamide-streptogramin A (*lsa*(*E*)). Virulence gene composition was different between the two isolates. BR-MHR218Efa harboured only two virulence genes involved in adherence (*acm* and *scm*). BR-MHR268Efe harboured eight complete virulence operons including three operons involved in adherence (Ace, Ebp pili, and EfaA), two operons involved in biofilm formation (BopD and Fsr), and three exoenzymes (gelatinase, hyaluronidase, SprE).

Conclusions: The genome sequences of the strains BR-MHR268Efe and BR-MHR218Efa will serve as a reference point for molecular epidemiological studies of mastitis-associated *E. faecalis* and *E. faecium*. Additionally, the findings will help understand the complex antimicrobial-resistance in livestock-assoiated *Enterococci*.

1. Introduction

Antimicrobial resistance is a global quintessential *One Health* dilemma that is interconnected within and across human, animal, and environmental health. Gram-negative and Gram-positive bacteria of multiple genera are important causative agents of bovine mastitis throughout the world. Mastitis is a complex, multiaetio-

* Corresponding author.
E-mail addresses: elzow005@gmail.com (M.E. El Zowalaty), bahanurr@bau.edu.bd (Md.B. Rahman).
Equal first authors.

https://doi.org/10.1016/j.jgar.2024.05.011

logical, and serious dairy cow disease involving udder and intramammary gland inflammation caused by infections from mastitis-causing pathogens [1]. Mastitis poses a risk to public health, veterinary health, and the farming industry worldwide. Mastitis causes devastating economic losses due to reduced milk production and quality, consequent milk withdrawal due to antibiotic use, treatment costs, and culling of diseased cows on dairy farms [2]. Enterococci are ubiquitous environmental bacteria capable of causing opportunistic infections in humans and many animals, including mastitis in dairy cows [3,4]. The detection of mastitis-causing and antimicrobial-resistant *Enterococcus faecalis* and *Enterococcus faecium* isolated from livestock and dairy farm environments has been reported worldwide [5-8]; however, there are very scarce data available on using whole-genome sequencing for the characterization of these mastitis-causing pathogens, including Enterococci.

Extensive use of antibiotics in the management of mastitis has resulted in the emergence and spread of antimicrobial and multidrug-resistant resistant *E. faecalis* and *E. faecium* [9,10].

The aetiologies, management, treatment, and physiological and molecular characterization of mastitis-causing pathogens, as well as the metagenomics of milk microbiota, were recently reported in Bangladesh [6,11]. Recently, we reported on the detection and genome sequences of two *Escherichia coli* strains: one strain was assigned to a novel sequence type 13054 and the other strain belonged to sequence type 101. Both strains were isolated from raw milk samples obtained from lactating cows infected with mastitis in Bangladesh [12].

Here we report on the draft genome sequences of *E. faecalis* and *E. faecium* strains isolated from raw milk samples obtained from July to August 2021 from mastitis-affected lactating cows in Bangladesh.

2. Methods

In the present study, milk samples were collected from 36- and 46-month-old female lactating Holstein Friesian (*Bos taurus taurus*) cows, as previously reported [13]. Briefly, cow udders were washed with clean water and dried, then the udder teats were rubbed with 70% ethanol. The first two strings were discarded, and a California mastitis test was performed to determine somatic cell counts in milk samples. Milk samples (10 mL) were collected in sterile tubes and samples were transported to the laboratory, maintaining a cold chain for further analysis. Somatic cell counts were performed using Lactoscan Combo's SCC (Milkotronic Ltd, Bulgaria) according to the manufacturer's protocol. Nutrient broth (10 mL) was inoculated with 500 µL of the milk sample, incubated at 37°C for 18 h, and subsequently streaked on *Enterococcus* agar plates (HiMedia). The inoculated plates were incubated at 37°C for 24 h and subcultured to isolate pure colonies. Pure single colonies were identified using matrix-assisted laser desorption ionisation time of flight (MALDI-TOF) mass spectrometry (MS) using a MALDI Biotyper (Bruker Daltonics, Bremen, Germany), and isolates with a log score ≥2 indicated species identification, as previously reported [14]. *Enterococcus* isolates were subjected to whole-genome sequencing as previously described [12].

DNA was extracted from overnight cultures grown in nutrient broth at 37°C using a genomic DNA Purification Kit (Promega, USA). Sequencing libraries were prepared using the Nextera XT library preparation kit (Illumina, USA) and sequenced on an Illumina NextSeq 550 using the NextSeq 500/550 High Output Kit v2.5 (300 cycles). Default parameters were used for all software, unless otherwise specified. Quality control was performed using the ASA^{3}P pipeline (v1.4.0) [15]. Assembly was performed using SPAdes v3.13.0 [16] integrated in ASA^{3}P. Contigs, excluding those smaller than 200 bp, were uploaded to the National Center for Biotechnology Information (NCBI) and annotated using the NCBI Prokaryotic Genome Annotation Pipeline v6.0 [17]. The sequencing, assembly, and annotation data of BR-MHR268Efe and MHR218Efa are summarized in Table 1. Multilocus sequence types (STs) were determined using PubMLST [18], the Homan scheme for *E. faecium* [19], and the Ruiz-Garbajosa scheme for *E. faecalis* [20]. Antimicrobial resistance genes were detected using Resfinder (v4.0) [21]. Virulence genes were detected using the VFDB database [22] included in ASA^{3}P. Core genome-based phylogeny was determined using Harvest Suite software tools [23]. The number of single nucleotide polymorphisms (SNPs) was determined using MEGA X [24] and the consensus sequences generated by Harvest Suite. Annotation of the core genome-based phylogenies was generated using ITOL v6 [25] and Inkscape 0.91 (https://inkscape.org/release/inkscape-0.91/?latest=1).

Table 1
Basic characteristics of the whole-genome sequencing, assemblies, annotation, and genes of *Enterococcus faecalis* strain BR-MHR218Efa and *Enterococcus faecium* strain BR-MHR268Efe

Parameter	BR-MHR218Efa	BR-MHR268Efe
No. of raw reads	9 438 233	9 307 778
Average read length (nt)	149	149
Average coverage (x)	909	816
No. of contigs >200 bp	118	17
N_{50} [bp]	70.213	305.353
Genome size (bp)	2 576 280	2 810 324
G+C content (%)	38	37
No. of genes (total)	2534	2653
No. of CDSs (with protein)	2372	2578
No. of genes (RNA)	61	54
No. of rRNAs (5S, 16S, 23S)	1, 1, 1	1, 1, 1
Complete	1, 1, 1	1, 1, 1
Partial	0, 0, 0	0, 0, 0
No. of tRNAs	54	47
No. of ncRNAs	4	4
No. of pseudogenes (total)	101	21

CDS: coding sequence, ncRNA: non-coding RNA, tRNA: transfer RNA.

3. Results

In the current study, a total of 423 randomly selected lactating cows were tested for the detection of *Enterococci* in milk samples. It was found that 44.68% (189/423) of the cows were mastitis positive, of which 17.49% (74/423) had clinical and 27.19% (115/423) had subclinical mastitis, as previously reported [13]. *Enterococcus* isolation was performed by culture methods using *Enterococcus* agar plates and presumptive isolates were subsequently confirmed using MALDI-TOF MS [14]. It was found that the prevalence rates of *E. faecalis* and *E. faecium* were 14.28% (27 out of 189 samples) and 6.35% (12 out of 189 samples), respectively, in the in the examined milk samples.

Table 2
Antibiotic resistance genes detected in *Enterococcus faecalis* strain BR-MHR218Efa and *Enterococcus faecium* strain BR-MHR268Efe in the present study

Antibiotic class	BR-MHR218Efa	BR-MHR268Efe
Aminoglycoside	*ant[6]-Ia, aph(3′)-III*	
Sulphonamide	*aac(6′)-II-like*	
Lincosamide	*lnu(B)*	
Macrolide	*erm(B)*	*lsa(A)-like*
Macrolide, lincosamide and streptogramin B	*msr(C)-like*	
Tetracycline	*tet(M)-like, tet(L)*	
Trimethoprim	*dfrG*	
Pleuromutilin-lincosamide-streptogramin A	*lsa(E)*	

Table 3
Virulence genes detected in *Enterococcus faecalis* strain BR-MHR218Efa and *Enterococcus faecium* strain BR-MHR268Efe in the present study

Virulence category	Virulence determinant	Genes present in isolates		Operon
		BR-MHR218Efa	BR-MHR268Efe	
Adherence	Acm (VF0419)	*acm*		Complete
	Scm (VF0418)	*scm*		Complete
	Ace (VF0355)		*ace*	Complete
	AS (VF0352)		*asa1*	Not complete
	Ebp pili (VF0538)		*srtC, ebpC, ebpA, ebpB*	Complete
	EfaA (VF0354)		*efaA*	Complete
Biofilm	BopD (VF0362)		*bopD*	Complete
	Fsr (VF0360)		*fsrA, fsrB, fsrC*	Complete
Exoenzyme	Gelatinase (VF0357)		*gelE*	Complete
	Hyaluronidase (VF0359)		*EF0818, EF3023*	Complete
	SprE (VF0358)		*sprE*	Complete
Immune modulation	Capsule (VF0361)		*cpsA, cpsB*	Not complete

BR-MHR218Efa and BR-MHR268Efe belonged to multilocus sequence types ST-190 and ST-22, respectively. Both sequence types appear to represent relatively rare sequence types, as only three ST-190 *E. faecium* and six ST-22 *E. faecalis* STs have been deposited in the PubMLST database.

E. faecium ST-190 has been isolated from meat chickens in Australia [26] as well as human infections in Portugal [27]. To the authors' knowledge, it has never before been detected in mastitis samples.

E. faecalis ST-22 has been isolated from mastitis samples [28], but also from other samples such as chicken meat and from human infections in Portugal [29]. To the authors' knowledge, *E. faecalis* ST-22 has not been detected in mastitis samples before the current study.

The antibiotic resistance genes detected in the two isolates differed greatly (Table 2). BR-MHR268Efe harboured only one antibiotic resistance gene encoding resistance towards macrolides (*lsa(A)*), while BR-MHR218Efa harboured ten different antibiotic resistance genes encoding resistance to aminoglycosides (*ant(6)-Ia, aph(3′)-III*), sulphonamides (*aac(6′)-II*), lincosamides (*lnu(B)*), macrolides (*erm(B)*), MLSB antibiotics (*msr(C)*), tetracyclines (*tet(M), tet(L)*), trimethoprim (*dfrG*) and pleuromutilin-lincosamide-streptogramin A (*lsa(E)*).

Virulence genes also differed greatly between the two isolates (Table 3). BR-MHR218Efa harboured only two virulence genes involved in adherence (*acm, scm*). BR-MHR268Efe harboured eight complete virulence operons (Table 3): three operons involved in adherence (Ace, Ebp pili, and EfaA), two operons involved in biofilm formation (BopD and Fsr), and three exoenzymes (gelatinase, gyaluronidase, and SprE).

As only a limited number of *E. faecium* ST-190 and *E. faecalis* ST-22 were present in the PubMLST database ($n = 1$ each), we used

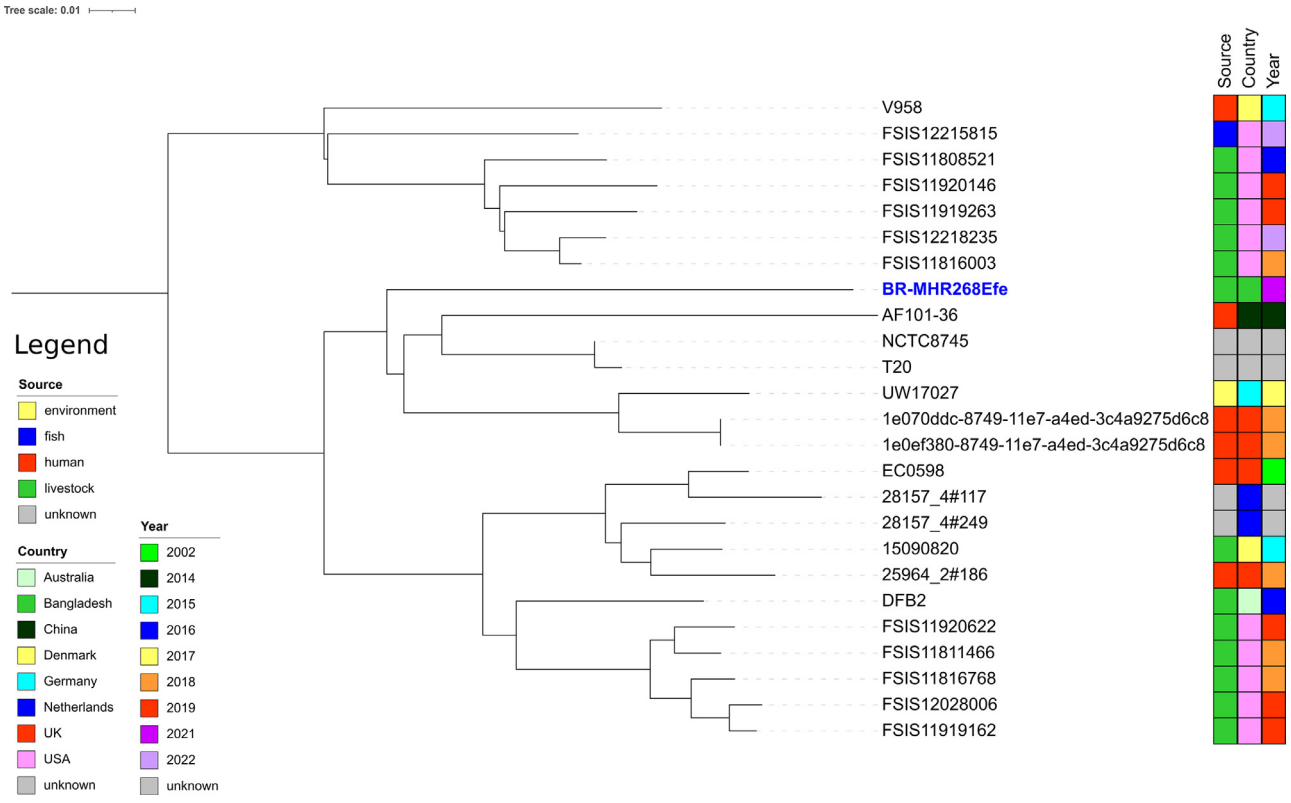

Fig. 1. Core genome-based analysis of *Enterococcus faecium* strain BR-MHR268Efe and all *Enterococcus faecium* ST-22 isolates publicly available in the National Center for Biotechnology Information assembly database.

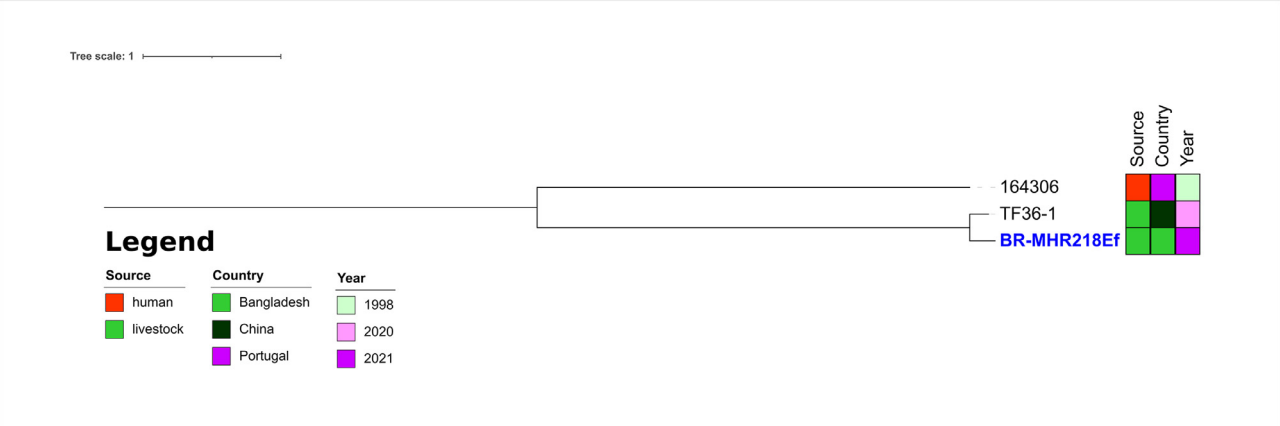

Fig. 2. Core-genome-based analysis of *Enterococcus faecalis* strain BR-MHR218Efa and all *Enterococcus faecalis* ST-190 isolates publicly available in the National Center for Biotechnology Information assembly database.

a different strategy to determine the closest relatives of the two isolates. All assemblies for *E. faecalis* (n = 7276) and *E. faecium* (n = 19868) were downloaded from NCBI (as of 13 July 2023) and analysed using ASA^{3}P to determine the multilocus sequence type. *E. faecalis* ST-22 (n = 24, supplementary Table A) and *E. faecium* ST-190 (n = 2, supplementary Table B) were detected and compared with BR-MHR218Efa and BR-MHR268Efe using core genome-based phylogenetic analysis.

The closest relative to BR-MHR268Efe was NCTC8745 (BioSample SAMEA1046663) from an unknown source (Fig. 1, Supplementary Table C), albeit the relatively high number of SNPs (n = 237) indicates a very distant genetic relationship. The closest relative to BR-MHR218Efa was TF36-1 (BioSample SAMN31232721) isolated from an unidentified source from a pig in China (Fig. 2, Supplementary Table D). The very high number of SNPs (n = 559) indicates that these isolates are not related.

4. Conclusions

Bovine mastitis is a significant zoonotic disease of serious global impact [30]. Mastitis has a zoonotic potential associated with shedding of bacteria and their toxins in unpasteurized milk, which may lead to potential health threats in humans and other animals [5,30]. In addition, antimicrobial resistance from bovine mastitis pathogens may lead to severe infections. The *E. faecium* and *Enterobacter* genus are members of the ESKAPE pathogens, which are among the main bacterial causative agents of antibiotic-resistant nosocomial infections [31,32] that have been designated “priority status” by the World Health Organization [33].

To the authors’ knowledge, this is the first report on whole-genome sequencing of mastitis-associated *Enterococci* species in Bangladesh. The present study represents important findings on the detection of mastitis-associated *Enterococci* species in dairy cows, which requires further extensive investigations. This report highlights the significance of continued genomic surveillance of mastitis-associated bacteria, which continue to pose a serious global threat to animal health and food security. Monitoring and genomic characterization of mastitis-associated *Enterococci* species in food-chain cattle and food-production environments will help to further understanding of its zoonotic potential, role in the spread of antimicrobial resistance, and pathogenesis. Furthermore, comprehensive genome analysis of mastitis-associated *Enterococci* species will help us to understand the genomic architecture, rearrangements, and movement of mobile genetic elements, virulence-associated genes, and antimicrobial resistance determinants. It will also help to elucidate their complex aetiology and ability to cause mastitis in udder-healthy cows.

Data availability

All isolates reported in this study were submitted to Public Databases for molecular typing and microbial genome diversity for curation and are publicly available in *Enterococcus faecalis* PubMLST and *Enterococcus faecium* PubMLST, under ID numbers 2346 and 4570, respectively. This whole-genome sequencing project has been deposited at DDBJ/ENA/GenBank under the BioProject number PRJNA716986, BioSample accession numbers SAMN26025964 and SAMN26025968, and GenBank accession numbers JALBGN000000000 and JALBGJ000000000 for BR-MHR218Efa and BR-MHR268Efe, respectively. The versions described in this paper are the first version. The sequences have been submitted to the Sequence Read Archive (SRA) under the accession numbers SRR18182113 and SRR18182109.

Ethics Statement

The study protocol entitled “Development of polyvalent mastitis vaccine and probiotics for prevention of mastitis in cows” under the project entitled “Polyvalent Vaccine Development for Mastitis in Dairy Cow” reference number AWEEC/BAU/2020(44) was approved by the Animal Welfare and Experimentation Ethics Committee, Bangladesh Agricultural University, Mymensingh-2202, Bangladesh.

Competing interests

None declared.

Acknowledgements

The whole-genome sequencing project was supported in part by the Bangladesh Academy of Sciences and the United States Department of Agriculture (Project ID: BAS-USDA LS-26/2020), the Bangladesh Agricultural University Research System (BAURES), and the Hessian Ministry of Higher Education, Research and Arts within the project HuKKH (Hessisches Universitaeres Kompetenzzentrum Krankenhaus Hygiene), Germany. The authors thank the National Center for Biotechnology Information (NCBI) GenBank submission staff for their help and support throughout genome upload, decontamination, and deposition processes. The authors thank Dr. Shakeel Mowlaboccus, PubMLST curator of the *E. faecium* and *E. faecalis* databases from the Antimicrobial Resistance and Infectious

Diseases Research Laboratory, the College of Science, Health, Engineering and Education, Murdoch University, Murdoch, Western Australia, Australia, for help and cooperation. The authors would also like to thank the anonymous reviewers for their comments and feedback, which significantly improved the manuscript.

Supplementary materials

Supplementary material associated with this article can be found, in the online version, at doi:10.1016/j.jgar.2024.05.011.

References

[1] Pascu C, Herman V, Iancu I, Costina L. Etiology of mastitis and antimicrobial resistance in dairy cattle farms in the western part of Romania. Antibiotics 2022;11:57. doi:10.3390/antibiotics11010057.
[2] Goulart DB, Mellata M. *Escherichia coli* mastitis in dairy cattle: etiology, diagnosis, and treatment challenges. Front Microbiol 2022;13:928346. doi:10.3389/fmicb.2022.928346.
[3] Gao X, Fan C, Zhang Z, Li S, Xu C, Zhao Y, et al. Enterococcal isolates from bovine subclinical and clinical mastitis: antimicrobial resistance and integron-gene cassette distribution. Microb Pathog 2019;129:82–7. doi:10.1016/j.micpath.2019.01.031.
[4] Kateete DP, Kabugo U, Baluku H, Nyakarahuka L, Kyobe S, Okee M, et al. Prevalence and antimicrobial susceptibility patterns of bacteria from milkmen and cows with clinical mastitis in and around Kampala, Uganda. PLoS One 2013;8(5):e63413. doi:10.1371/journal.pone.0063413.
[5] El Zowalaty ME, Lamichhane B, Falgenhauer L, Mowlaboccus S, Zishiri OT, Forsythe S, et al. Antimicrobial resistance and whole genome sequencing of novel sequence types of *Enterococcus faecalis, Enterococcus faecium*, and *Enterococcus durans* isolated from livestock. Sci Rep 2023;13:18609. doi:10.1038/s41598-023-42838-z.
[6] Bag MAS, Arif M, Riaz S, Khan MSR, Islam MS, Punom SA, et al. Antimicrobial resistance, virulence profiles, and public health significance of *Enterococcus faecalis* isolated from clinical mastitis of cattle in Bangladesh. Biomed Res Int 2022;2022:8101866. doi:10.1155/2022/8101866.
[7] Kim HJ, Youn HY, Kang HJ, Moon JS, Jang YS, Song KY, et al. Prevalence and virulence characteristics of *Enterococcus faecalis* and *Enterococcus faecium* in bovine mastitis milk compared to bovine normal raw milk in South Korea. Animals (Basel) 2022;12(11):1407. doi:10.3390/ani12111407.
[8] Santos PR, Kraus RB, Ladeira SL, Pereira GM, Cunha KF, Palhares KE, et al. Resistance profile and biofilm production of *Enterococcus* spp., *Staphylococcus* sp., and *Streptococcus* spp. from dairy farms in southern Brazil. Braz J Microbiol 2023;54(2):1217–29. doi:10.1007/s42770-023-00929-z.
[9] Różańska H, Lewtak-Piłat A, Kubajka M, Weiner M. Occurrence of enterococci in mastitic cow's milk and their antimicrobial resistance. J Vet Res 2019;63(1):93–7. doi:10.2478/jvetres-2019-0014.
[10] Erbas G, Parin U, Turkyilmaz S, Ucan N, Ozturk M, Kaya O. Distribution of antibiotic resistance genes in *Enterococcus* spp. isolated from mastitis bovine milk. Acta Vet 2016;66:336–46. doi:10.1515/acve-2016-0029.
[11] Hoque MN, Istiaq A, Clement RA, Sultana M, Crandall KA, Siddiki AZ, et al. Metagenomic deep sequencing reveals association of microbiome signature with functional biases in bovine mastitis. Sci Rep 2019;9:13536. doi:10.1038/s41598-019-49468-4.
[12] Rahman MH, El Zowalaty ME, Falgenhauer L, Khan MFR, Alam J, Popy NN, et al. Draft genome sequences of two clinical mastitis-*associated Escherichia coli* strains, of sequence type 101 and novel sequence type 13054, isolated from dairy cows in Bangladesh. Microbiol Resour Announce 2023;12(8):e0016623. doi:10.1128/mra.00166-23.
[13] Rahman MH, El Zowalaty ME, Falgenhauer E, Khan MFR, Alam J, Popy NN, et al. Molecular identification and whole genome sequence analyses of methicillin-resistant and mastitis-associated *Staphylococcus aureus* sequence types 6 and 2454 isolated from dairy cows. J Genomics 2024;12:19–25. doi:10.7150/jgen.90833.
[14] Nonnemann B, Lyhs U, Svennesen L, Kristensen KA, Klaas, Pedersen K. Bovine mastitis bacteria resolved by MALDI-TOF mass spectrometry. J Dairy Sci 2018;102:2515–24.
[15] Schwengers O, Hoek A, Fritzenwanker M, Falgenhauer L, Hain T, Chakraborty T, et al. ASA3P: an automatic and scalable pipeline for the assembly, annotation and higher-level analysis of closely related bacterial isolates. PLoS Comput Biol 2020;16(3):e1007134. doi:10.1371/journal.pcbi.1007134.
[16] Bankevich A, Nurk S, Antipov D, Gurevich AA, Dvorkin M, Kulikov AS, et al. SPAdes: a new genome assembly algorithm and its applications to single-cell sequencing. J Comput Biol 2012;19(5):455–77. doi:10.1089/cmb.2012.0021.
[17] Tatusova T, DiCuccio M, Badretdin A, Chetvernin V, Nawrocki EP, Zaslavsky L, et al. NCBI prokaryotic genome annotation pipeline. Nucleic Acids Res 2016;44:6614–24. doi:10.1093/nar/gkw569.
[18] Jolley KA, Bray JE, Maiden MCJ. Open-access bacterial population genomics: BIGSdb software, the PubMLST.org website and their applications. Wellcome Open Res 2018;3:124. doi:10.12688/wellcomeopenres.14826.1.
[19] Homan WL, Tribe D, Poznanski S, Li M, Hogg G, et al. Multilocus sequence typing scheme for *Enterococcus faecium*. J Clin Microbiol 2002;40(6):1963–71. doi:10.1128/JCM.40.6.1963-1971.2002.
[20] Ruiz-Garbajosa P, Bonten MJ, Robinson DA, Top J, Nallapareddy SR, et al. Multilocus sequence typing scheme for *Enterococcus faecalis* reveals hospital-adapted genetic complexes in a background of high rates of recombination. J Clin Microbiol 2006;44(6):2220–8. doi:10.1128/JCM.02596-05.
[21] Bortolaia V, Kaas RS, Ruppe E, Roberts MC, Schwarz S, Cattoir V, et al. ResFinder 4.0 for predictions of phenotypes from genotypes. J Antimicrob Chemother 2020;75(12):3491–500. doi:10.1093/jac/dkaa345.
[22] Liu B, Zheng D, Zhou S, Chen L, Yang J. VFDB 2022: a general classification scheme for bacterial virulence factors. Nucleic Acids Res 2022;50(D1):D912–17. doi:10.1093/nar/gkab1107.
[23] Treangen TJ, Ondov BD, Koren S, Phillippy AM. The Harvest suite for rapid core-genome alignment and visualization of thousands of intraspecific microbial genomes. Genome Biol 2014;15(11):524. doi:10.1186/s13059-014-0524-x.
[24] Kumar S, Stecher G, Li M, Knyaz C, Tamura K. MEGA X: molecular evolutionary genetics analysis across computing platforms. Mol Biol Evol 2018;35(6):1547–9. doi:10.1093/molbev/msy096.
[25] Letunic I, Bork P. Interactive tree of life (iTOL) v3: an online tool for the display and annotation of phylogenetic and other trees. Nucleic Acids Res 2016;44:W242–5. doi:10.1093/nar/gkw290.
[26] O'Dea M, Sahibzada S, Jordan D, Laird T, Lee T, Hewson K, et al. Genomic, antimicrobial resistance, and public health insights into *Enterococcus* spp. from Australian chickens. J Clin Microbiol 2019;57(8):e00319. doi:10.1128/JCM.00319-19.
[27] Freitas AR, Novais C, Tedim AP, Francia MV, Baquero F, Peixe L, et al. Microevolutionary events involving narrow host plasmids influences local fixation of vancomycin-resistance in *Enterococcus* populations. PLoS One 2013;8(3):e60589. doi:10.1371/journal.pone.0060589.
[28] Werner G, Fleige C, Fessler AT, Timke M, Kostrzewa M, Zischka M, et al. Improved identification including MALDI-TOF mass spectrometry analysis of group D streptococci from bovine mastitis and subsequent molecular characterization of corresponding *Enterococcus faecalis* and *Enterococcus faecium* isolates. Vet Microbiol 2012;160(1–2):162–9. doi:10.1016/j.vetmic.2012.05.019.
[29] Freitas AR, Novais C, Ruiz-Garbajosa P, Coque TM, Peixe L. Clonal expansion within clonal complex 2 and spread of vancomycin-resistant plasmids among different genetic lineages of *Enterococcus faecalis* from Portugal. J Antimicrob Chemother 2009;63(6):1104–11. doi:10.1093/jac/dkp103.
[30] Maity S, Ambatipudi K. Mammary microbial dysbiosis leads to the zoonosis of bovine mastitis: a One-Health perspective. FEMS Microbiol Ecol 2021;97(1):fiaa241. doi:10.1093/femsec/fiaa241.
[31] De Oliveira DMP, Forde BM, Kidd TJ, Harris PNA, Schembri MA, Beatson SA, et al. Antimicrobial resistance in ESKAPE pathogens. Clin Microbiol Rev 2020;33(3) e00181-19. doi:10.1128/CMR.00181-19.
[32] Denissen J, Reyneke B, Waso-Reyneke M, Havenga B, Barnard T, Khan S, et al. Prevalence of ESKAPE pathogens in the environment: antibiotic resistance status, community-acquired infection and risk to human health. Int J Hyg Environ Health 2022;244:114006. doi:10.1016/j.ijheh.2022.114006.
[33] Tacconelli E, Carrara E, Savoldi A, Harbarth S, Mendelson M, Monnet DL, Pulcini C, Kahlmeter G, Kluytmans J, Carmeli Y, Ouellette M, Outterson K, Patel J, Cavaleri M, Cox EM, Houchens CR, Grayson ML, Hansen P, Singh N, Theuretzbacher U, Magrini N. WHO Pathogens Priority List Working Group. Discovery, research, and development of new antibiotics: the WHO priority list of antibiotic-resistant bacteria and tuberculosis. Lancet Infect Dis 2018;18(3):318–27. doi:10.1016/S1473-3099(17)30753-3.